DISCRETE HOLOMORPHICITY AND QUANTIZED AFFINE ALGEBRAS

Y. IKHLEF, R. WESTON, M. WHEELER, AND P. ZINN-JUSTIN

Abstract. We consider non-local currents in the context of quantized affine algebras, following the construction introduced by Bernard and Felder. In the case of $U_q(A_1^{(1)})$ and $U_q(A_2^{(2)})$, these currents can be identified with configurations in the six-vertex and Izergin–Korepin nineteen-vertex models. Mapping these to their corresponding Temperley–Lieb loop models, we directly identify non-local currents with discretely holomorphic loop observables. In particular, we show that the bulk discrete holomorphicity relation and its recently derived boundary analogue are equivalent to conservation laws for non-local currents.

1. Introduction

Discretely holomorphic observables are correlations functions in a two-dimensional lattice model which satisfy a discrete version of the Cauchy–Riemann (CR) equations. In the context of the Ising model, lattice fermions with this type of property were first described in [13]. More recently, the discrete CR equations were used by Smirnov as a basic tool to study rigorously the scaling properties of Ising interfaces [27]. They were then exploited in the Probability literature, to obtain mathematical proofs of several Coulomb-gas results. For instance, still in the Ising model, this approach yielded the scaling limit of domain walls and Fortuin-Kasteleyn cluster boundaries [10, 16], and the spin and energy correlation functions [9]. For self-avoiding walks, it provided a rigorous way to determine the bulk [14] and boundary [4] connectivity constants, and it has also proved very useful for numerical purposes [5].

In the meantime, some discretely holomorphic observables have been identified in other 2D lattice models, including the $\mathbb{Z}_N$ clock model [24] and the dense [25] and dilute [18] Temperley–Lieb (TL) loop models. These observables are essentially non-local, either because they include disorder operators (in spin models), or because they are defined in terms of an open path attached to the boundary (in loop models). In all the known examples, it was observed that the discrete holomorphicity condition is satisfied precisely when the Boltzmann weights are such that the model is integrable [24, 18]. Recently, this statement was also extended to the boundary Boltzmann weights [17, 11]. These observed relations between the notions of discrete holomorphicity and integrability have been explored further recently [1], but they still call for a more systematic understanding: this is the object of the present work.

An obvious starting point for this is to try and construct discrete holomorphic observables from the underlying symmetries of a the lattice model. This idea is very reminiscent of the construction of non-local conserved currents $\psi(z)$ in lattice models possessing a quantum group symmetry [6]. Indeed, in that context, $\psi(z)$ is non-local because it includes a path connecting z to a reference point, in a similar way to disorder operators in spin systems. Moreover, the conservation equation for the current is a linear relation between the values of ψ at the points adjacent to a given vertex, like the discrete holomorphicity condition. These resemblances [15] between discrete holomorphic observables and conserved currents can actually be made more precise.

The present paper is based on a simple observation: in the case of an affine quantum group symmetry, the conservation equation of currents can be written as a discrete holomorphicity condition on the rhombic lattice with opening angle α, provided an appropriate relation between α and the spectral parameter is introduced.

We thus consider two simple loop models where discretely holomorphic observables – which we shall call for short *loop observables* – are known: the dense and dilute Temperley–Lieb models on the square lattice. Using the mapping of these loop models onto vertex models possessing $U_q(A_1^{(1)})$ and $U_q(A_2^{(2)})$ symmetry respectively, we construct the conserved currents, and show that they map to the loop observables identified previously. This analysis is extended to boundary observables in the case of general diagonal integrable boundary conditions.

This point of view explains the somewhat mysterious observation of [24, 18] that discrete holomorphicity somehow "linearizes" the Yang–Baxter equation by providing us with a linear equation for integrable Boltzmann weights. Indeed, from our point of view, this linearization procedure is nothing but Jimbo's interpretation [20] of the R-matrix of an integrable model as a representation of the universal R-matrix of a quantized affine algebra, which by definition satisfies such a linear relation, as will be explained below.

The plan of the paper is as follows. In § 2, we review the construction of conserved currents introduced in [6] and expose a general identity for the adjoint action in this context. § 3 reviews the correspondence between the six- and nineteen-vertex models and the dense and dilute Temperley–Lieb loop models respectively. In particular, we show that the integrable weights can be obtained by solving the intertwining relations, which are linear equations in the Boltzmann weights assigned to loop model tiles. In § 4, we use the mapping between vertex and loop models to express the currents as loop observables, satisfying the discrete Cauchy–Riemann equations. § 5 extends the work of [6] to systems with a boundary, and focuses on the interpretation of current conservation at the boundary. § 6 introduces boundary tiles into the dense and dilute Temperley–Lieb loop models. Integrable weights for these tiles are obtained by solving linear equations which are the boundary analogue of the intertwining relations. In § 7, we express our currents (which satisfy current conservation at the boundary) as loop observables obeying boundary discrete Cauchy–Riemann equations. In § 8, we use the Coulomb-gas approach to present the continuum limit of the loop observables. We conclude in § 9.

2. Vertex models, currents and quantized affine algebras

2.1. **Vertex models.** In this section, we recall how vertex models in statistical mechanics can be defined in terms of Boltzmann weights which are given as intertwiners of representations of quantized affine algebras. More specifically, we will consider the case in which we have a quantized affine algebra U with a spectral parameter dependent module V_z. We denote the associated representation as (π_z, V_z) where $\pi_z : U \to \mathrm{End}(V_z)$ and additionally use the notation $\pi_{z_1,\dots,z_M} = \pi_{z_1} \otimes \cdots \otimes \pi_{z_m}$ for tensor products of such representations.

Assuming that $V_z \otimes V_w$ is generically irreducible, the R-matrix $R(z/w) : V_z \otimes V_w \to V_z \otimes V_w$ that defines the vertex model is given as the solution (unique up to overall normalization) of the linear relation

$$R(z/w)\, \pi_{z,w}(\Delta(X)) = \pi_{z,w}(\Delta'(X))\, R(z/w) \tag{1}$$

for all $X \in U$; where $\Delta : U \to U \otimes U$ is the coproduct, $\Delta(X) = \sum X_1 \otimes X_2$, and Δ' the coproduct with the order of the tensor product reversed, $\Delta'(X) = \sum X_2 \otimes X_1$. We represent the R-matrix pictorially by

$R(z/w) =$ 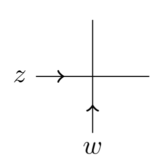

The arrows drawn on the lines are purely to indicate "time flow": reading an equation from right to left corresponds to reading along a line in the direction of the arrows.

Let us define the multiple coproduct $\Delta^{(L)} : U \to U^{\otimes(L)}$ by $\Delta^{(L+1)} = (\Delta \otimes 1)\Delta^{(L)}$ and $\Delta^{(2)} = \Delta$. The monodromy matrix $T^{(L)}(z; w_1, \dots, w_L) : V_z \otimes V_{w_1} \otimes \cdots \otimes V_{w_L} \to V_z \otimes V_{w_1} \otimes \cdots \otimes V_{w_L}$ is defined as

$$T^{(L)}(z; w_1, \dots, w_L) = R_{0L}(z/w_L) \dots R_{01}(z/w_1)\,,$$

where the subscripts on R-matrices indicate the evaluation modules in which they act, *i.e.*, $0 \leftrightarrow V_z$, $1, \dots, L \leftrightarrow V_{w_1}, \dots, V_{w_L}$. Its graphical representation is

$T^{(L)}(z; w_1, \dots, w_L) =$ 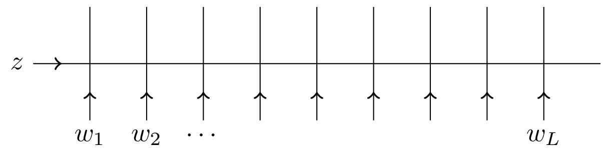

Until specified otherwise, all lines will be oriented up/right in what follows, so that we shall omit arrows on pictures.

By vertically concatenating M monodromy matrices $T^{(L)}(z_i; w_1, \dots, w_L)$, $1 \le i \le M$, one obtains a rectangular lattice Ω of width L and height M. Each horizontal (resp. vertical) line of this lattice is oriented from left to right (resp. bottom to top), and denotes the vector space V_{z_i} (resp. V_{w_j}).

To simplify the discussion, from now on we will work on a horizontally and vertically homogeneous lattice, by assuming that all horizontal (resp. vertical) lines carry the same evaluation parameter $z_i = z$ (resp. $w_j = w$). We will be interested in operators that act on the vector spaces encoded by the lattice, which graphically corresponds to the insertion of a "node" at an edge. The edges of the lattice will be denoted by coordinates pairs $(x \pm \frac{1}{2}, t)$ or $(x, t \pm \frac{1}{2})$, where (x, t) is a vertex of Ω, and x (resp. t) is the horizontal (resp. vertical) coordinate.

Typically, one is interested in the case where the left/right boundaries of this lattice are fixed in some way. In such a case, each row of the lattice becomes an operator in $V_{w_1} \otimes \cdots \otimes V_{w_L} := V_1 \otimes \cdots \otimes V_L$ that we will rather loosely call the "one-row transfer matrix" $\mathbf{T}$. We will use this construction below, despite the fact that for now we do not discuss the boundary conditions explicitly.

2.2. **Hopf algebras and graphical relations.** Following Bernard and Felder [6], we consider a set of elements $\{J_a, \Theta_a{}^b, \widehat{\Theta}^a{}_b\}$, $a, b = 1, \dots, n$, of a Hopf algebra U. The elements $\Theta_a{}^b$ and $\widehat{\Theta}^a{}_b$ are assumed to be inverses of each other:

$$\Theta_a{}^b \widehat{\Theta}^c{}_b = \delta_{a,c} \quad \text{and} \quad \widehat{\Theta}^b{}_a \Theta_b{}^c = \delta_{a,c} \tag{2}$$

(where here and subsequently repeated indices are summed over) while the coproduct Δ and antipode S of all elements have the form:

$$\Delta(J_a) = J_a \otimes 1 + \Theta_a{}^b \otimes J_b \qquad\qquad S(J_a) = -\widehat{\Theta}^b{}_a J_b \tag{3a}$$

$$\Delta(\Theta_a{}^c) = \Theta_a{}^b \otimes \Theta_b{}^c \qquad\qquad S(\Theta_a{}^b) = \widehat{\Theta}^b{}_a \tag{3b}$$

$$\Delta(\widehat{\Theta}^a{}_c) = \widehat{\Theta}^a{}_b \otimes \widehat{\Theta}^b{}_c \qquad\qquad S(\widehat{\Theta}^a{}_b) = \Theta_b{}^a. \tag{3c}$$

It is also useful to define $\widehat{J}_a := -\widehat{\Theta}^b{}_a J_b$, which has the coproduct and antipode

$$\Delta(\widehat{J}_a) = \widehat{J}_b \otimes \widehat{\Theta}^b{}_a + 1 \otimes \widehat{J}_a \qquad\qquad S(\widehat{J}_a) = \widehat{\Theta}^c{}_b J_c \Theta_a{}^b. \tag{3d}$$

Given two elements in $\{J_a\}$, say J_1 and J_2, $J_1 + J_2$ can be trivially added to the set $\{J_a\}$ in such a way that (3a–3d) still hold. It is a little less obvious that the same is true of $J_1 J_2$, with appropriately defined sets $\{\Theta_a{}^b\}$ and $\{\widehat{\Theta}^a{}_b\}$. Therefore we only need to specify a set $\{J_a\}$ that generates U as a unital algebra.

The R-matrix, $R : U \otimes U \to U \otimes U$, switches the order of tensor products in the coproduct: namely, $R\Delta(X_a) = \Delta'(X_a)R$ for all $X_a \in U$. Applying this to the coproducts in (3a–3d) gives, respectively

$$R(J_a \otimes 1 + \Theta_a{}^b \otimes J_b) = (1 \otimes J_a + J_b \otimes \Theta_a{}^b)R \tag{4a}$$

$$R(\Theta_a{}^b \otimes \Theta_b{}^c) = (\Theta_b{}^c \otimes \Theta_a{}^b)R \tag{4b}$$

$$R(\widehat{\Theta}^a{}_b \otimes \widehat{\Theta}^b{}_c) = (\widehat{\Theta}^b{}_c \otimes \widehat{\Theta}^a{}_b)R \tag{4c}$$

$$R(\widehat{J}_b \otimes \widehat{\Theta}^b{}_a + 1 \otimes \widehat{J}_a) = (\widehat{\Theta}^b{}_a \otimes \widehat{J}_b + \widehat{J}_a \otimes 1)R\,. \tag{4d}$$

Suppose now that we have a representation (π, V) of the Hopf algebra U. In the spirit of [6], we can represent $\pi(J_a)$, $\pi(\Theta_a{}^b)$ and $\pi(\widehat{\Theta}^a{}_b)$ by the following pictures (from now on we always discuss representations of U, and so suppress the appearance of the π):

$J_a =$ 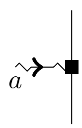

, $\Theta_a{}^b =$ 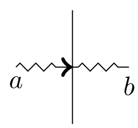

, $\widehat{\Theta}^a{}_b =$ 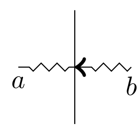

where the vertical line denotes the vector space V with an upward arrow that we have suppressed, and subscripts (resp. superscripts) correspond to incoming (resp. outgoing) arrows. The operator $\widehat{J}_a$ has the graphical representation

$\widehat{J}_a = -$ 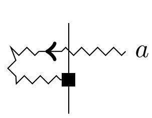

that we simplify to $\widehat{J}_a =$ 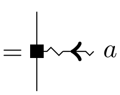

so that a connection of a wavy line to a solid line from the right (compared to the direction of time) corresponds to the insertion of the operator $\widehat{J}_a$.

Using these notations, the equations listed have natural graphical meanings. Relation (2) is expressed graphically by

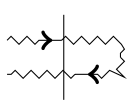 $=$ 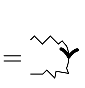 and 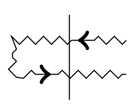 $=$ 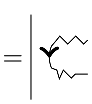

and the first coproduct relation (4a) is equivalent to

(5a) 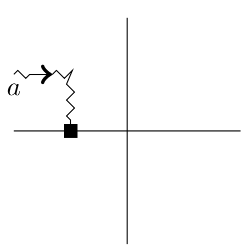

$+$ 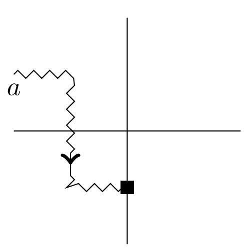

$=$ 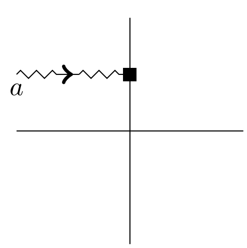

$+$ 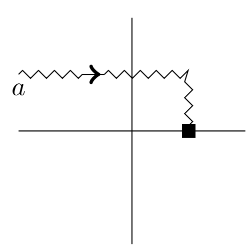

$R(J_a \otimes 1)$ $\qquad$ $R(\Theta_a{}^b \otimes J_b)$ $\qquad$ $(1 \otimes J_a)R$ $\qquad$ $(J_b \otimes \Theta_a{}^b)R$

where we recall that the "time flow" is south-west to north-east. Similarly, for "tail operators" one has

(5b)

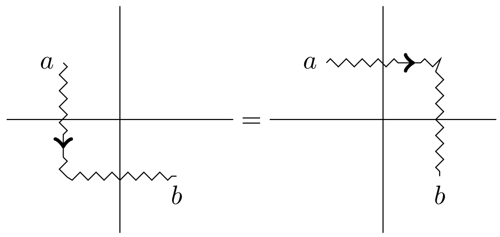

$$R({\Theta_a}^c \otimes {\Theta_c}^b) \qquad ({\Theta_c}^b \otimes {\Theta_a}^c)R$$

which means one can move the tail freely across vertices. The remaining equations (4c–4d) have analogous the graphical equivalents, but the tails now enter from the right:

(5c)

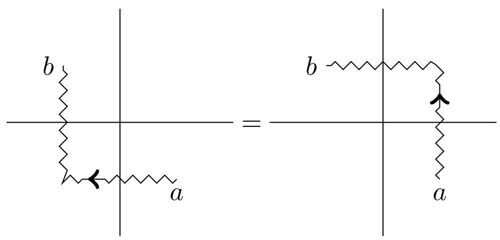

$$R(\widehat{\Theta}^b{}_c \otimes \widehat{\Theta}^c{}_a) \qquad (\widehat{\Theta}^c{}_a \otimes \widehat{\Theta}^b{}_c)R$$

(5d)

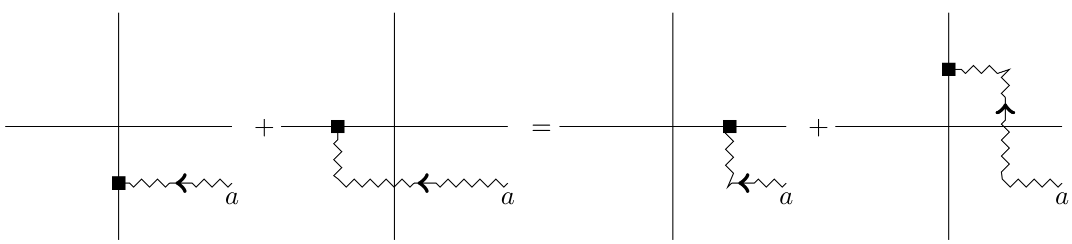

$$R(1 \otimes \widehat{J}_a) \qquad R(\widehat{J}_b \otimes \widehat{\Theta}^b{}_a) \qquad (\widehat{J}_a \otimes 1)R \qquad (\widehat{\Theta}^b{}_a \otimes \widehat{J}_b)R$$

2.3. **Non-local currents and conservation laws in the bulk.** Continuing along the lines of [6], we act with the repeated coproduct $\Delta^{(L)}$ on the elements of U to define non-local currents. By iterating the coproduct in (3a), we obtain

$$\mathbf{J}_a := \Delta^{(L)}(J_a) = \sum_{x=1}^{L} j_a^{(t)}(x), \quad j_a^{(t)}(x) := \delta_{a,a_1} {\Theta_{a_1}}^{a_2} \otimes \cdots \otimes {\Theta_{a_{x-1}}}^{a_x} \otimes J_{a_x} \otimes 1 \otimes \cdots \otimes 1\,. \tag{6}$$

The object thus constructed, $\mathbf{J}_a$, is the charge associated with the time component $j_a^{(t)}(x)$ of a non-local current. Acting on a tensor product $V_1 \otimes \cdots \otimes V_L$, we have the graphical representation

$j_a^{(t)}(x) =$ 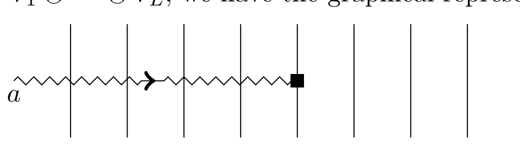

where each solid line corresponds to a space V_i (the tensor product is ordered from left to right, as in the corresponding algebraic expression). If $V_i \simeq \mathbb{C}^d$ as below, then each solid line will carry an index in

$\{1, \ldots, d\}$, and each wavy line an index $a \in \{1, \ldots, n\}$. The intersection of a wavy line and a solid line is a ${\Theta_{a_i}}^{a_{i+1}}$ acting on the solid line.

We want to reinterpret (4a) (or its graphical equivalent, (5a)) as a discrete current conservation for a vector field $(j_a^{(x)}, j_a^{(t)})$, where the index x corresponds to horizontal direction and the index t to vertical direction. This leads us to define $j_a^{(x)}(x)$, $x \in \mathbb{Z} + 1/2$, as the insertion of a dot on the horizontal edge $[x - 1/2, x + 1/2]$ (with a tail attached, one half-step up and then to the left). If one wants to define $j_a^{(x)}$ as an operator on $V_1 \otimes \cdots \otimes V_L$, one needs to "embed" it inside a transfer matrix: *i.e.*, letting $\mathbf{T}$ be the one-row transfer matrix (recall that the boundary conditions on the left/right are left undetermined in this section), we define

$$\mathbf{T}^{1/2} j_a^{(x)}(x) \mathbf{T}^{1/2} =$$

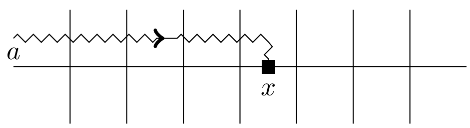

Adding a tail to all terms in (5a) which extends all the way to the left, we can straighten it using (5b). Assuming that the tail commutes with the left boundary, we find

$$j_a^{(x)}(x - 1/2, t) - j_a^{(x)}(x + 1/2, t) + j_a^{(t)}(x, t - 1/2) - j_a^{(t)}(x, t + 1/2) = 0 \tag{7}$$

where in the operator formalism, the time evolution of any operator $\mathcal{O}$ is given by $\mathcal{O}(t) = \mathbf{T}^t \mathcal{O} \mathbf{T}^{-t}$. Equation (7) expresses the conservation of the current $(j_a^{(x)}, j_a^{(t)})$ that we have defined.

Summing (7) over x results in the conservation law for the associated global charge $\mathbf{J}_a$ (6), up to boundary terms:

$$\mathbf{J}_a(t + 1/2) - \mathbf{J}_a(t - 1/2) = j_a^{(x)}(1/2, t) - j_a^{(x)}(L + 1/2, t)\,. \tag{8}$$

If we depict the charge $\mathbf{J}_a$ by

$$\mathbf{J}_a =$$

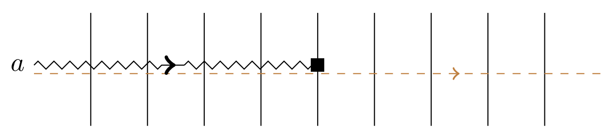

where the oriented dashed line represents summation over the position of the node (*i.e.*, discrete integration), then (8) has the graphical interpretation

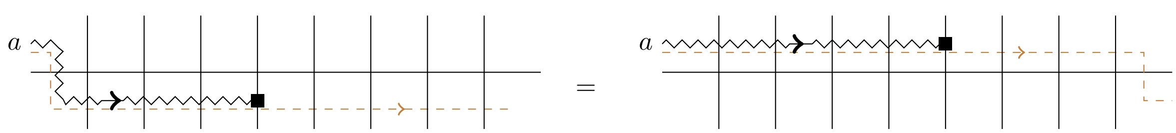

In this paper, we shall be mostly concerned with the "local" relation (7) and not so much with the global relation (8). Note however that even the former relation is not strictly local because of the tails; we therefore shall have to pay attention to the boundary conditions to the left when applying it in what follows.

It is the purpose of this paper to relate (7) to the so-called discrete holomorphicity condition.

2.4. **Adjoint action.** A detailed discussion of the action of U on local fields and of its adjoint action can be found in §2.4 and 2.5 of [6]. Here we summarize some relevant facts. Let us write the general coproduct as

$$\Delta(X) = \sum X^{(1)} \otimes X^{(2)}\,,$$

for any $X \in U$. The adjoint action of a Hopf algebra is defined by

$$\mathrm{ad}_X\,(Y) := \sum X^{(1)}\; Y\; S\left(X^{(2)}\right)\,.$$

In the case of elements of the form J_a, whose coproduct and antipode are given by (3a), this means that

$$\mathrm{ad}_{J_a}(J_b) = J_a J_b - \Theta_a{}^c J_b \widehat{\Theta}^d{}_c J_d \,.$$

The natural action of J_a on $\mathbf{J}_b$, viewed as an operator on $V_1 \otimes \cdots \otimes V_L$, is obtained by applying $\Delta^{(L)}$:

$$\Delta^{(L)}\left[\mathrm{ad}_{J_a}(J_b)\right] = \sum_{x=1}^{L} A_a \left[j_b^{(t)}(x,t) \right] \,,$$

where A_a on the r.h.s. is the action of J_a on local fields, and is best described graphically:

(9) $$A_a \left[j_b^{(t)}(x,t) \right] =$$ 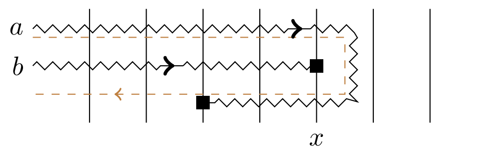

Once again, dashed lines denote discrete contour integration.

A similar procedure can be carried out for the action on the other component $j_b^{(x)}$ of currents. In this way, one can organize various currents as multiplets of U (or of subalgebras of U). In general, starting from some generators J_a, the adjoint action of the whole of U produces a large subspace inside U. Note however that in the case of quantized affine algebras, to be discussed now, the Serre relations imply that the module generated by the adjoint action of a $U_q(A_1) := U_q(sl_2)$ subalgebra on some other Chevalley generator is finite-dimensional.

We now apply the formalism of previous sections to particular quantized affine algebras.

2.5. **Quantized affine algebras.** In this paper we always take U to be a quantized affine algebra $U_q(\mathfrak{g})$ corresponding to a rank 1 affine Lie algebra $\mathfrak{g}$. Let $\mathcal{A}_{ij}$ denote the entries of the generalized Cartan matrix for $U_q(\mathfrak{g})$, and let d_i be integers such that $d_i \mathcal{A}_{ij} = d_j \mathcal{A}_{ji}$, whose greatest common divisor is 1. Then the Chevalley presentation of $U_q(\mathfrak{g})$ is given in terms of the generators $\{E_i, F_i, T_i\}$, $i \in \{0, 1\}$, satisfying the list of relations[1]

$$T_i T_i^{-1} = T_i^{-1} T_i = 1, \quad [T_i, T_j] = 0 \,, \tag{10}$$

$$T_i E_j T_i^{-1} = q^{d_i \mathcal{A}_{ij}} E_j, \quad T_i F_j T_i^{-1} = q^{-d_i \mathcal{A}_{ij}} F_j, \quad [E_i, F_j] = \delta_{ij} \frac{T_i - T_i^{-1}}{q^{d_i} - q^{-d_i}} \,, \tag{11}$$

$$\sum_{k=0}^{1-\mathcal{A}_{ij}} (-)^k \begin{bmatrix} 1-\mathcal{A}_{ij} \\ k \end{bmatrix}_{q^{d_i}} (E_i)^{1-\mathcal{A}_{ij}-k} E_j (E_i)^k = 0 \,, \tag{12}$$

$$\sum_{k=0}^{1-\mathcal{A}_{ij}} (-)^k \begin{bmatrix} 1-\mathcal{A}_{ij} \\ k \end{bmatrix}_{q^{d_i}} (F_i)^{1-\mathcal{A}_{ij}-k} F_j (F_i)^k = 0 \,, \tag{13}$$

where we use the notation

$$\begin{bmatrix} m \\ n \end{bmatrix}_q := \frac{(q^m - q^{-m}) \dots (q^{m-n+1} - q^{-m+n-1})}{(q^n - q^{-n}) \dots (q - q^{-1})} \,.$$

The coproduct of these generators is taken to be

$$\Delta(E_i) = E_i \otimes 1 + T_i \otimes E_i \,, \qquad \Delta(F_i) = F_i \otimes T_i^{-1} + 1 \otimes F_i \,, \qquad \Delta(T_i) = T_i \otimes T_i \,.$$

[1] For a review of quantized affine algebras see [8].

It is also useful for our purposes to introduce the modified generators $\bar{E}_i := q^{d_i} T_i F_i$, whose coproduct takes the more convenient form:

$$\Delta(\bar{E}_i) = \bar{E}_i \otimes 1 + T_i \otimes \bar{E}_i \,.$$

The correspondence between these generators and the Hopf algebra elements $J_a, \Theta_a{}^b, \widehat{\Theta}^a{}_b$ introduced in § 2.2 is immediate. For $a = 0, 1$ we set: $J_a = E_a, \bar{E}_a$, their coproduct being of the form of (3a); $\Theta_a{}^b = \delta_{a,b} T_a$ (resp. $\widehat{\Theta}^a{}_b = \delta_{a,b} T_a^{-1}$) their coproduct being of the form (3b) (resp. (3c)); $\widehat{J}_a = F_a$, their coproduct being of the form (3d)).

In the following subsections we describe the two quantized affine algebras which will interest us in this paper, as well as the representations to be considered.

2.5.1. *The case $U = U_q(A_1^{(1)})$.* The first case of interest to us is $U_q(A_1^{(1)})$, for which the generalized Cartan matrix is given by

$$\begin{pmatrix} \mathcal{A}_{00} & \mathcal{A}_{01} \\ \mathcal{A}_{10} & \mathcal{A}_{11} \end{pmatrix} = \begin{pmatrix} 2 & -2 \\ -2 & 2 \end{pmatrix}$$

and $d_0 = d_1 = 1$. The representation (π_z, V_z) is taken as the level-zero fundamental (principal) evaluation representation $V_z = \mathbb{C}^2[[z]]$

$$\pi_z(E_0) = \begin{pmatrix} 0 & 0 \\ z & 0 \end{pmatrix} \qquad \pi_z(\bar{E}_0) = \begin{pmatrix} 0 & z^{-1} \\ 0 & 0 \end{pmatrix} \qquad \pi_z(T_0) = \begin{pmatrix} q^{-1} & 0 \\ 0 & q \end{pmatrix}$$

$$\pi_z(E_1) = \begin{pmatrix} 0 & z \\ 0 & 0 \end{pmatrix} \qquad \pi_z(\bar{E}_1) = \begin{pmatrix} 0 & 0 \\ z^{-1} & 0 \end{pmatrix} \qquad \pi_z(T_1) = \begin{pmatrix} q & 0 \\ 0 & q^{-1} \end{pmatrix} .$$

The R-matrix $R(z)$ is given by

$$R(z) = \left(\begin{array}{cc|cc} qz - q^{-1}z^{-1} & 0 & 0 & 0 \\ 0 & z - z^{-1} & q - q^{-1} & 0 \\ \hline 0 & q - q^{-1} & z - z^{-1} & 0 \\ 0 & 0 & 0 & qz - q^{-1}z^{-1} \end{array}\right) , \tag{14}$$

which gives the weights of the 6-vertex model in the principal gradation.

2.5.2. *The case $U = U_q(A_2^{(2)})$.* The second case which we study is $U_q(A_2^{(2)})$, for which the generalized Cartan matrix is

$$\begin{pmatrix} \mathcal{A}_{00} & \mathcal{A}_{01} \\ \mathcal{A}_{10} & \mathcal{A}_{11} \end{pmatrix} = \begin{pmatrix} 2 & -4 \\ -1 & 2 \end{pmatrix}$$

and $d_0 = 1$, $d_1 = 4$. The representation (π_z, V_z) is now $V_z = \mathbb{C}^3[[z, z^\ell]]$ with

$$\pi_z(E_0) = z^{1-\ell}\varphi(q) \begin{pmatrix} 0 & 0 & 0 \\ 1 & 0 & 0 \\ 0 & q & 0 \end{pmatrix} \qquad \pi_z(E_1) = z^{+2\ell} \begin{pmatrix} 0 & 0 & 1 \\ 0 & 0 & 0 \\ 0 & 0 & 0 \end{pmatrix}$$

$$\pi_z(\bar{E}_0) = z^{\ell-1}\varphi(q) \begin{pmatrix} 0 & q^{-1} & 0 \\ 0 & 0 & 1 \\ 0 & 0 & 0 \end{pmatrix} \qquad \pi_z(\bar{E}_1) = z^{-2\ell} \begin{pmatrix} 0 & 0 & 0 \\ 0 & 0 & 0 \\ 1 & 0 & 0 \end{pmatrix}$$

$$\pi_z(T_0) = \begin{pmatrix} q^{-2} & 0 & 0 \\ 0 & 1 & 0 \\ 0 & 0 & q^2 \end{pmatrix} \qquad \pi_z(T_1) = \begin{pmatrix} q^4 & 0 & 0 \\ 0 & 1 & 0 \\ 0 & 0 & q^{-4} \end{pmatrix} ,$$

where $\varphi(q) = (q+q^{-1})^{1/2}$, and ℓ is an arbitrary constant which we will fix later. The R-matrix is

$$R(z) = \left(\begin{array}{ccc|ccc|ccc}
\omega_{14} & & & & & & & & \\
& \omega_{10} & & \omega_5 & & & & & \\
& & \omega_{16} & & \omega_8 & & \omega_{19} & & \\
\hline
& \omega_2 & & \omega_{12} & & & & & \\
& & \omega_7 & & \omega_1 & & \omega_6 & & \\
& & & & & \omega_{13} & & \omega_3 & \\
\hline
& & \omega_{18} & & \omega_9 & & \omega_{17} & & \\
& & & & & \omega_4 & & \omega_{11} & \\
& & & & & & & & \omega_{15}
\end{array}\right), \tag{15}$$

where the entries are given by

$$\begin{aligned}
\omega_1 &= (z-z^{-1})(q^3z+q^{-3}z^{-1}) + (q^2-q^{-2})(q^3+q^{-3}) \\
\omega_2 = \omega_4 &= z^{-\ell}(q^2-q^{-2})(q^3z+q^{-3}z^{-1}) \\
\omega_3 = \omega_5 &= z^{+\ell}(q^2-q^{-2})(q^3z+q^{-3}z^{-1}) \\
\omega_6 = \omega_8 &= -q^{+2}z^{+\ell}(q^2-q^{-2})(z-z^{-1}) \\
\omega_7 = \omega_9 &= +q^{-2}z^{-\ell}(q^2-q^{-2})(z-z^{-1}) \\
\omega_{10} = \omega_{11} = \omega_{12} = \omega_{13} &= (z-z^{-1})(q^3z+q^{-3}z^{-1}) \\
\omega_{14} = \omega_{15} &= (q^2z-q^{-2}z^{-1})(q^3z+q^{-3}z^{-1}) \\
\omega_{16} = \omega_{17} &= (z-z^{-1})(qz+q^{-1}z^{-1}) \\
\omega_{18} &= z^{-2\ell}(q^2-q^{-2})[(q^2+q^{-2})qz^2-(q-q^{-1})q^{-2}] \\
\omega_{19} &= z^{+2\ell}(q^2-q^{-2})[(q^2+q^{-2})q^{-1}z^{-2}+(q-q^{-1})q^2]\,.
\end{aligned}$$

These coincide with the Boltzmann weights of the Izergin–Korepin 19-vertex model, up to factors of $z^{\pm\ell}$ which come from the fact that we have not yet fixed the gradation.

3. From vertex models to loop models

In this section we review the loop/vertex model connection for $U_q(A_1^{(1)})$ and $U_q(A_2^{(2)})$ models in the bulk. Until this stage, our analysis has been on a lattice Ω with an arbitrary angle between horizontal and vertical lines. We now specify our domain further, by considering a rhombic lattice of definite angle α, which we will ultimately relate to the ratio of the spectral parameters z/w. We also draw the dual lattice using dotted lines:

(16) $R =$ 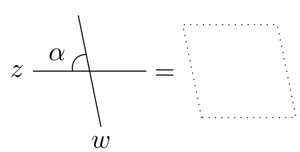

where the edges of an elementary "plaquette" (elementary rhombus of the dual lattice) are of unit length.

3.1. **The dense Temperley–Lieb model and the $U_q(A_1^{(1)})$ vertex model.**

The dense Temperley–Lieb model is defined by assigning weights a and b to the following two local configurations of a rhombus with top-left lattice angle α:

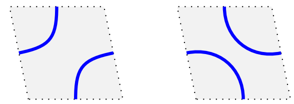

a $\qquad$ b

and weight τ to closed loops in a given lattice configuration C. Thus, C is assigned the Boltzmann weight

$$W(C) = a^{N_a(C)}\, b^{N_b(C)}\, \tau^{N_\ell(C)}\,, \tag{17}$$

where $N_a(C)$ (resp. $N_b(C)$) is the number of plaquettes of weight a (resp. b), and $N_\ell(C)$ is the number of closed loops in C.

Let us now recall how [3] these weights are related to those of the six-vertex model. Firstly, we identify

$$\tau = -(q+q^{-1}), \qquad q := -e^{2\pi i\nu}. \tag{18}$$

We then associate the above configurations with operators A, $B : V\otimes V \to V \otimes V$ (acting SW-NE), with $V = \mathbb{C}\,|\uparrow\rangle \oplus \mathbb{C}\,|\downarrow\rangle$. This is done by dressing each configuration with arrows and reading off the associated weight $e^{i\nu\delta}$ associated with total turning angle δ.[2] In this way we obtain

$$A := \left(\begin{array}{cc|cc} 1 & 0 & 0 & 0 \\ 0 & e^{2i\nu\alpha} & 0 & 0 \\ \hline 0 & 0 & e^{-2i\nu\alpha} & 0 \\ 0 & 0 & 0 & 1 \end{array}\right), \qquad B := \left(\begin{array}{cc|cc} 0 & 0 & 0 & 0 \\ 0 & e^{-2i\nu(\pi-\alpha)} & 1 & 0 \\ \hline 0 & 1 & e^{2i\nu(\pi-\alpha)} & 0 \\ 0 & 0 & 0 & 0 \end{array}\right), \tag{19}$$

in the basis $\{|\uparrow\uparrow\rangle, |\uparrow\downarrow\rangle, |\downarrow\uparrow\rangle, |\downarrow\downarrow\rangle\}$. The $\check{R}$-matrix is then the linear combination of these operators, dressed by their respective weights:

$$\check{R} := PR = a\ A + b\ B = \left(\begin{array}{cc|cc} a & 0 & 0 & 0 \\ 0 & e^{2i\nu\alpha}a + e^{-2i\nu(\pi-\alpha)}b & b & 0 \\ \hline 0 & b & e^{-2i\nu\alpha}a + e^{2i\nu(\pi-\alpha)}b & 0 \\ 0 & 0 & 0 & a \end{array}\right). \tag{20}$$

3.2. **Six-vertex model weights from intertwining relations.** It is well known that the commutant of the quantized algebra $U_q(A_1)$ acting on a tensor product of two-dimensional representations is the Temperley–Lieb algebra [19]. This suggests that the two terms A and B in (20) are intertwiners for the subalgebra $\langle E_1, \bar{E}_1, T_1\rangle \cong U_q(A_1)$. Indeed, one can check that

$$\begin{cases} A\, \pi_{z,w}(\Delta(X)) = \pi_{w,z}(\Delta(X))\, A \\ B\, \pi_{z,w}(\Delta(X)) = \pi_{w,z}(\Delta(X))\, B\,, \end{cases} \qquad X = E_1, \bar{E}_1, T_1\,, \tag{21}$$

provided the following relation holds between angle and spectral parameters: $z/w = e^{-2i\nu\alpha}$. Notice that the equation for $X = T_1$ is automatically satisfied, since both A and B preserve the total magnetization.

Moreover, imposing that $\check{R}$ commute in a similar way with the action of E_0, $\bar{E}_0$ fixes the ratio a/b, say

$$a = q\,x - q^{-1}x^{-1}, \qquad b = x - x^{-1}, \qquad x := z/w. \tag{22}$$

Substituting these values for the weights into (20), we recover the 6-vertex R-matrix (14).

Remark: The explicit connection of the operators (19) with the usual generators of the Temperley–Lieb algebra is as follows. On a strip of width L, the Temperley–Lieb algebra with generators $\{g_1, \dots, g_L\}$ satisfies the list of relations

$$\begin{array}{rcl} g_j g_{j\pm1} g_j &=& g_j \\ g_j^2 &=& \tau g_j \\ g_j g_k &=& g_k g_j, \quad \text{if } |j-k|>1. \end{array} \tag{23}$$

[2] We assume, as shown on the pictures, that the loop lines enter/leave *orthogonally* to the sides of the rhombus.

The generator g_j acts non-trivially on spaces at positions j and $j+1$, and the weights for a plaquette at this position are encoded in the $\check{\mathcal{R}}$-matrix $\check{\mathcal{R}}_{j,j+1} = a\,\mathbf{1} + b\,g_j$. Both the identity $\mathbf{1}$ and TL generator g_j have well known graphical interpretations, as a 45 degree rotation and deformation of the tiles above into squares.

Consequently, we expect that $\check{R}$ and $\check{\mathcal{R}}$ are related by a simple gauge transformation (corresponding to the passage from principal gradation to homogeneous gradation), which is indeed the case; we find that

$$\check{\mathcal{R}} = \mathcal{U}^{-1}\ \check{R}\,\mathcal{U}'\,, \qquad \mathcal{U} := w^{\sigma^z/2} \otimes z^{\sigma^z/2}\,, \qquad \mathcal{U}' := z^{\sigma^z/2} \otimes w^{\sigma^z/2}\,,$$

since under this transformation the two terms in $\check{R}$ become

$$\mathcal{U}^{-1}\ A\,\mathcal{U}' = \mathbf{1}\,, \qquad \mathcal{U}^{-1}\ B\,\mathcal{U}' = \begin{pmatrix} 0 & 0 & 0 & 0 \\ 0 & -q^{-1} & 1 & 0 \\ 0 & 1 & -q & 0 \\ 0 & 0 & 0 & 0 \end{pmatrix}\,,$$

where the second term is the well-known spin-$\frac{1}{2}$ representation of g_j.

3.3. The dilute Temperley–Lieb model and the $U_q(A_2^{(2)})$ vertex model.

The dilute Temperley–Lieb model (or O(n) model) is defined by the plaquette configurations:

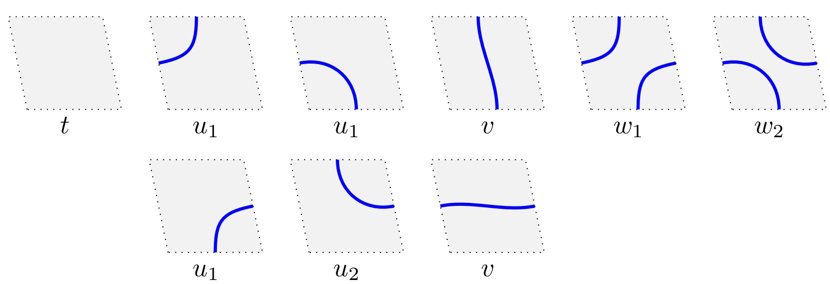

with corresponding weights shown beneath the configurations. The Boltzmann weight of a configuration C is given by

$$W(C) = t^{N_t(C)}\ u_1^{N_{u_1}(C)} u_2^{N_{u_2}(C)} w_1^{N_{w_1}(C)} w_2^{N_{w_2}(C)} \tau^{N_\ell(C)}\,,$$

where N_α is the number of plaquettes of type α, and N_ℓ is the number of closed loops. In a similar way to the dense case, we introduce the parameters

$$\tau = -(q^4 + q^{-4}), \qquad q := e^{i\pi(\frac{\nu}{2} - \frac{1}{4})}.$$

Now we identify the configurations with operators $T, U_1', U_1'', U_2', U_2'', V', V'', W_1, W_2 : V \otimes V \to V \otimes V$, where $V = \mathbb{C}^3 = \mathbb{C}\,|{\uparrow}\rangle \oplus \mathbb{C}\,|0\rangle \oplus \mathbb{C}\,|{\downarrow}\rangle$. We dress lines in the plaquette with arrows and associate them with $|{\uparrow}\rangle$ or $|{\downarrow}\rangle$, we identify missing lines with $|0\rangle$, and collect an associated weight $e^{i\nu\delta}$ for the total turning angle δ. To save space, we will not write down the explicit form of the resulting operators.

The $\check{R}$-matrix is, as before, the linear combination of all operators dressed by their Boltzmann weights. In the basis $\{|\uparrow\uparrow\rangle, |\uparrow 0\rangle, |\uparrow\downarrow\rangle, |0\uparrow\rangle, |00\rangle, |0\downarrow\rangle, |\downarrow\uparrow\rangle, |\downarrow 0\rangle, |\downarrow\downarrow\rangle\}$, it is given by

$$\check{R} = t\ T + u_1\ (U_1' + U_1'') + u_2\ (U_2' + U_2'') + v\ (V' + V'') + w_1\ W_1 + w_2\ W_2 = \tag{24}$$

$$\left(\begin{array}{ccc|ccc|ccc}
w_1 & 0 & 0 & 0 & 0 & 0 & 0 & 0 & 0 \\
0 & u_1 e^{i\nu\alpha} & 0 & v & 0 & 0 & 0 & 0 & 0 \\
0 & 0 & (w_1 + w_2 e^{-2i\nu\pi})e^{2i\nu\alpha} & 0 & u_2 e^{-i\nu(\pi-\alpha)} & 0 & w_2 & 0 & 0 \\
\hline
0 & v & 0 & u_1 e^{-i\nu\alpha} & 0 & 0 & 0 & 0 & 0 \\
0 & 0 & u_2 e^{-i\nu(\pi-\alpha)} & 0 & t & 0 & u_2 e^{i\nu(\pi-\alpha)} & 0 & 0 \\
0 & 0 & 0 & 0 & 0 & u_1 e^{i\nu\alpha} & 0 & v & 0 \\
\hline
0 & 0 & w_2 & 0 & u_2 e^{i\nu(\pi-\alpha)} & 0 & (w_1 + w_2 e^{2i\nu\pi})e^{-2i\nu\alpha} & 0 & 0 \\
0 & 0 & 0 & 0 & 0 & v & 0 & u_1 e^{-i\nu\alpha} & 0 \\
0 & 0 & 0 & 0 & 0 & 0 & 0 & 0 & w_1
\end{array}\right)$$

3.4. **Nineteen-vertex model weights from intertwining relations.** In analogy with the dense TL case, we wish to identify the plaquette operators as intertwiners of the subalgebra $\langle E_1, \bar{E}_1, T_1\rangle$. We find that

$$Y\,\pi_{z,w}(\Delta(X)) = \pi_{w,z}(\Delta(X))\,Y\,, \qquad X = E_1, \bar{E}_1, T_1\,, \quad Y = T, U_1', U_1'', U_2', U_2'', V', V'', W_1, W_2\,,$$

provided we set $(z/w)^{2\ell} = e^{-2i\nu\alpha}$. Furthermore, imposing that

$$\check{R}\ \pi_{z,w}(\Delta(X)) = \pi_{w,z}(\Delta(X))\ \check{R} \qquad X = E_0, \bar{E}_0, T_0\,,$$

determines the Boltzmann weights up to normalization:

$$\begin{aligned}
t &= (x - x^{-1})(q^3 x + q^{-3}x^{-1}) + (q^2 - q^{-2})(q^3 + q^{-3}) \\
u_1 &= (q^2 - q^{-2})(q^3 x + q^{-3}x^{-1}) \\
u_2 &= i(q^2 - q^{-2})(x - x^{-1}) \\
v &= (x - x^{-1})(q^3 x + q^{-3}x^{-1}) \\
w_1 &= (q^2 x - q^{-2}x^{-1})(q^3 x + q^{-3}x^{-1}) \\
w_2 &= (x - x^{-1})(qx + q^{-1}x^{-1})\,,
\end{aligned}$$

where we have again set $x := z/w$. Inserting these values for the weights into (24), we recover the 19-vertex R-matrix (15).

4. Discrete holomorphicity in the bulk

The goal of the present section is to connect (7) to discrete holomorphicity. To do so, we must finally specify our boundary conditions. In all cases to be considered, we shall choose "reflecting" boundary conditions, in which adjacent edges on the boundary are paired by a common loop (or are empty, which is allowed in the dilute TL model). The only exception to this rule will be two (or one, in the dilute case) boundary edges from which an open, unpaired loop propagates.

The reason for making this choice is that these are simple boundary conditions for which the boundary trivially commutes with the tail operators T_0, T_1, allowing us to apply (7). Indeed, our results extend to any choice of boundaries for which the tail operators satisfy this property. In particular, we wish to emphasise that our results *do not require integrable boundary conditions.*

The discussion of integrable boundaries, and the associated boundary discrete holomorphicity, is deferred to §5–7.

4.1. **Application to the dense loop model.**

4.1.1. *Loop observables associated to E_0 and $\bar{E}_0$.* Let us now consider the insertion on the lattice of the current e_0 associated to the operator E_0. We want to translate this insertion into the language of loops. We consider a model in which all loops are closed except one open path γ that connects two fixed boundary defects. In the vertex model, this is simply done by setting free boundary conditions for the two boundary defects. An example of such a configuration is shown below.

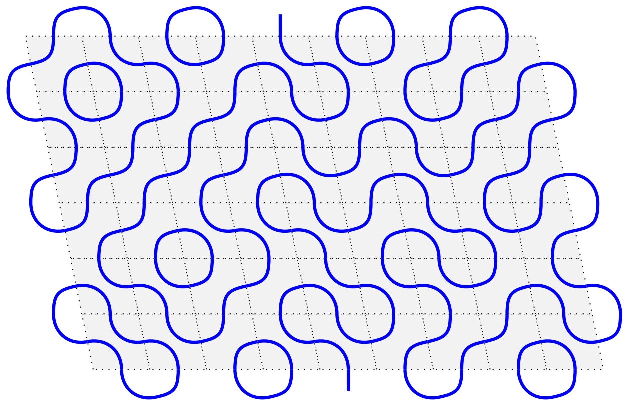

The important observation is that if the marked edge on which E_0 sits belongs to a closed loop, then the contribution is necessarily zero because of conservation of $u(1)$ charge. Graphically,

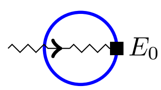

$= 0$, and
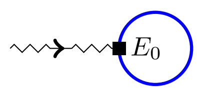

$= 0\,.$

To be precise, we have included the tail in these equations, but in fact the tail has an irrelevant contribution, since it is diagonal in the evaluation representation we are using. In subsequent pictures, the node marking will always correspond to insertion of E_0, and the wavy line to T_0. We conclude that in order to have a non-zero contribution, the marked edge must lie on the open path γ, and that the latter, whose orientation we had left unspecified so far, must be incoming at both boundaries:

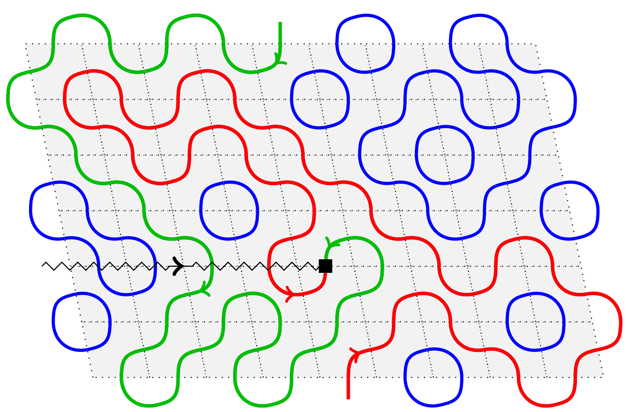

We first discuss $e_0^{(t)}$, *i.e.*, insertion on a horizontal edge of a plaquette, as on the picture above. We have $\pi_w(E_0) = w\sigma^-$, and the Boltzmann weight $W(C)$ is the same as in (17). The open path γ however has an additional factor $e^{2i\nu\theta(C)}$ where $\theta(C)$ is the angle spanned by the portion of γ between a boundary entry point and the insertion of E_0 (the red or green line) – the two angles are equal. In fact it is easy to see that $\theta(C) = \pi k(C)$ where $k(C)$ is an integer whose parity is fixed by the relative locations of marked edge and boundary entry points of the arc (on the example $k(C) = 2$). Finally, there is a contribution from the tail of $q^{-\sigma^z}$ (wavy line). It is easy to check that if k is even, red and green lines each cross (algebraically) the wavy line $k/2$ times, whereas if k is odd the red line crosses it $\lfloor k/2 \rfloor$ times and the green line $\lceil k/2 \rceil$ times. In both cases we find that this produces a factor $q^{k(C)}$. Using $q = e^{i\pi(2\nu-1)}$ and putting everything together we find

$$\left\langle e_0^{(t)}(x,t) \right\rangle = \frac{w}{Z} \sum_{C|(x,t)\in\gamma} W(C)\; e^{i(4\nu-1)\theta(C)}\,,$$

where we use the notation $\langle \mathcal{O} \rangle$ for the expectation value of an operator $\mathcal{O}$, and Z is the partition function, $Z = \sum_C W(C)$.

Now let us apply the same reasoning to $e_0^{(x)}$, for which a typical configuration is shown below:

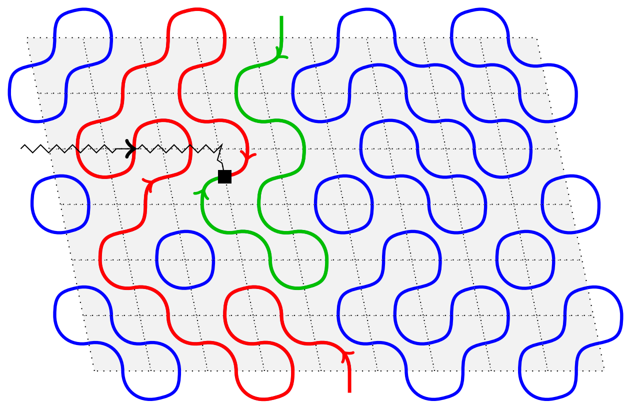

First we have a factor z. Then we have a factor from the angle $e^{2i\nu\theta}$ where this time $\theta = -\alpha + k\pi$ where k has fixed parity (on the example, $k=-1$). Finally, the tail crosses algebraically the red line $\lfloor k/2 \rfloor$ times, and the green line $\lceil k/2 \rceil$ times. In total we get $e^{2i\nu\theta} q^{(\theta+\alpha)/\pi} = e^{i(4\nu-1)\theta} e^{i(2\nu-1)\alpha}$,[3] or

$$\left\langle e_0^{(x)}(x,t) \right\rangle = \frac{z\; e^{i(2\nu-1)\alpha}}{Z} \sum_{C|(x,t)\in\gamma} W(C)\; e^{i(4\nu-1)\theta(C)}\,.$$

Note that $z\; e^{2i\nu\alpha} = w$. Therefore, if we define a function on the edges of the lattice

$$\phi_0(x,t) := w^{-1} \begin{cases} e_0^{(t)}(x,t), & (x,t) \in \mathbb{Z} \times (\mathbb{Z} + \frac{1}{2}) \\ e^{i\alpha} e_0^{(x)}(x,t), & (x,t) \in (\mathbb{Z} + \frac{1}{2}) \times \mathbb{Z}\,, \end{cases}$$

then we have

$$\langle \phi_0(x,t) \rangle = \frac{1}{Z} \sum_{C|(x,t)\in\gamma} W(C)\; e^{i(4\nu-1)\theta(C)}\,,$$

where $\theta(C)$ is the angle spanned by the open path γ from one boundary to (x,t).

Furthermore, the current conservation equation (7) for $j_a = e_0$ is

$$e_0^{(x)}(x-1/2,t) - e_0^{(x)}(x+1/2,t) + e_0^{(t)}(x,t-1/2) - e_0^{(t)}(x,t+1/2) = 0\,. \tag{25}$$

Rewriting (25) in terms of $\phi_0(x,t)$ we find

$$\phi_0(x,t-1/2) + e^{i(\pi-\alpha)}\phi_0(x+1/2,t) - e^{i(\pi-\alpha)}\phi_0(x-1/2,t) - \phi_0(x,t+1/2) = 0\,, \tag{26}$$

[3]If we instead defined $q = e^{i\pi(2\nu+1)}$ we would obtain the total factor $e^{i(4\nu-1)\theta}e^{i(2\nu+1)\alpha}$, leading to an observable which is discretely anti-holomorphic. There is no preferred definition for q, since exactly half of the observables are anti-holomorphic regardless of which choice we make.

which is precisely the discrete holomorphicity condition around a plaquette of the type:

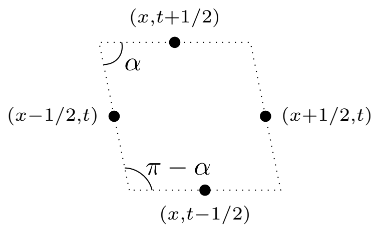

$$(x,t) \in \mathbb{Z}^2 \,.$$

This equality is valid at the operator level, *i.e.*, when inserted in an arbitrary correlation function $\langle \cdots \rangle$.

Note that ϕ_0 is exactly the lattice holomorphic observable identified in [25, 18]: we have shown here that this observable can be obtained by the construction of conserved currents associated to the $U_q(A_1^{(1)})$ symmetry of [6].

Everything can be repeated with $\bar{E}_0$ instead of E_0. This leads to the conjugate observable

$$\langle \bar{\phi}_0(x,t) \rangle = \frac{1}{Z} \sum_{C \mid (x,t) \in \gamma} W(C)\ e^{-i(4\nu-1)\theta(C)} \,,$$

which therefore satisfies an antiholomorphicity condition.

4.1.2. *Loop observables associated to E_1 and $\bar{E}_1$.* There is a simpler observable, obtained by considering E_1. We use the same type of boundary conditions as above; the whole discussion goes through, except for the following modifications. Compared to E_0, the arrows on the open path γ are inverted, but the tail is inverted as well (it is made of $q^{+\sigma^z}$). The result is that the tail and the angle factor almost compensate; for $e_1^{(t)}$ we find using the exact same reasoning that

$$\left\langle e_1^{(t)}(x,t) \right\rangle = \frac{w}{Z} \sum_{C \mid (x,t) \in \gamma} W(C)\ e^{-i\theta(C)} \,.$$

Note that $e^{-i\theta} = (-1)^k$ is independent of the configuration and simply measures the flux of γ through the marked edge (*i.e.*, the only configurations that contribute to $\langle e_1^{(t)} \rangle$ are those for which the average flux is nonzero, that is, where the open path goes through the marked edge). Similarly, for $e_1^{(x)}$ one finds $e^{-2i\nu\theta} q^{(\theta+\alpha)/\pi} = e^{-i\theta} e^{i(2\nu-1)\alpha}$, so

$$\left\langle e_1^{(x)}(x,t) \right\rangle = \frac{z\ e^{i(2\nu-1)\alpha}}{Z} \sum_{C \mid (x,t) \in \gamma} W(C)\ e^{-i\theta(C)} \,.$$

Again the same miracle happens in that $z e^{2i\nu\alpha} = w$. Note that the conservation law for e_1 is the obvious conservation of the flux of γ through a plaquette.

Finally, we define

$$\phi_1(x,t) := w^{-1} \begin{cases} e_1^{(t)}(x,t), & (x,t) \in \mathbb{Z} \times (\mathbb{Z} + \frac{1}{2}) \\ e^{i\alpha} e_1^{(x)}(x,t), & (x,t) \in (\mathbb{Z} + \frac{1}{2}) \times \mathbb{Z} \,, \end{cases}$$

and we have

$$\langle \phi_1(x,t) \rangle = \frac{1}{Z} \sum_{C \mid (x,t) \in \gamma} W(C)\ e^{-i\theta(C)} \,,$$

with the discrete holomorphicity equation

$$\phi_1(x,t-1/2) + e^{i(\pi-\alpha)} \phi_1(x+1/2,t) - e^{i(\pi-\alpha)} \phi_1(x-1/2,t) - \phi_1(x,t+1/2) = 0 \,. \tag{27}$$

Note that since E_1 commutes with each loop plaquette separately, *cf.* (21), the equation above is actually valid for each individual configuration of the loop model.

Similarly, insertion of $\bar{E}_1$ leads to the antiholomorphic observable

$$\langle \bar{\phi}_1(x,t) \rangle = \frac{1}{Z} \sum_{C|(x,t)\in\gamma} W(C)\ e^{+i\theta(C)}\,.$$

In all cases of observables, we observe that the different Borel subalgebras (E operators versus $\bar{E}$ operators) correspond to different chiralities from the point of view of Conformal Field Theory.

4.1.3. *A remark on local observables.* Note that the model also possesses a local observable, although its meaning is not transparent in the loop language. Write $T_i = q^{H_i}$, so that in the representation we use, $\pi_z(H_1) = -\pi_z(H_0) = \sigma^z$. The coproduct of H_i is the usual Lie algebra coproduct $\Delta H_i = H_i \otimes 1 + 1 \otimes H_i$, so that the corresponding current $h^{(x)} = h_1^{(x)} = -h_0^{(x)}$ and $h^{(t)} = h_1^{(t)} = -h_0^{(t)}$ does not carry a "tail", *i.e.*, is local. In the vertex language, $\langle h^{(x)}(x,t) \rangle$ simply gives the average orientation of the arrow sitting on the edge (x,t), and similarly for $h^{(t)}$. This observable should not be confused with the flux observable associated to E_1 or $\bar{E}_1$.

4.2. **Application to the dilute loop model.**

4.2.1. *Loop observables associated to E_0 and $\bar{E}_0$.* Consider the dilute Temperley–Lieb loop model on the lattice Ω described in § 2.1, with empty boundary conditions on all sides, except for one boundary site which is pointing inwards. The reason for this choice is that in the representation considered in § 2.5, the operator E_0 turns a spin $\uparrow$ into 0, or a 0 into $\downarrow$. Therefore, in the loop model, inserting $E_0(x,t)$ forces the path γ to go from the boundary defect to (x,t). For definiteness, we place the boundary defect at the bottom, say at $(x_d, 1/2)$. Consider firstly the case where the operator sits on a horizontal edge, $e_0^{(t)}$:

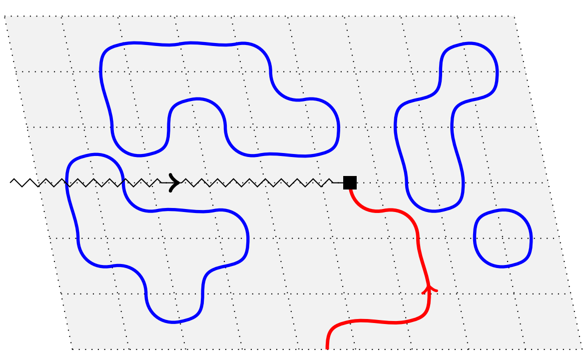

For the open path γ, we get the following factors. Denote the total winding angle of γ by θ. It is an integer multiple of π: $\theta = k\pi$ (however we do not know anything about the parity of k this time because in the dilute model the v-tiles are parity-changing). Then $e_0^{(t)}$ gets a factor $e^{i\nu\theta}$ from the local turns. Also, it is obvious that this loop crosses the tail (algebraically) $\lfloor k/2 \rfloor$ times. This produces a factor of $q^{2\lfloor k/2 \rfloor}$ from the tail (since the tail is comprised of T_0 operators). Also, the terms with k odd get a factor q from the matrix element of E_0. The final expression for the time-component of the current $e_0^{(t)}$ is

$$\left\langle e_0^{(t)}(x,t) \right\rangle = \frac{\varphi(q) w^{1-\ell}}{Z} \left(\sum_{\substack{C|\gamma:(x_d,1/2)\to(x,t) \\ k \text{ even}}} e^{i(\frac{\nu}{2}-\frac{1}{4})k\pi} + \sum_{\substack{C|\gamma:(x_d,1/2)\to(x,t) \\ k \text{ odd}}} q\ e^{i(\frac{\nu}{2}-\frac{1}{4})(k-1)\pi} \right) W(C)\ e^{i\nu k\pi}\,,$$

which can be combined into a single summation

$$\left\langle e_0^{(t)}(x,t)\right\rangle = \frac{\varphi(q)w^{1-\ell}}{Z} \sum_{C|\gamma:(x_d,1/2)\to(x,t)} W(C)\ e^{i(\frac{3\nu}{2}-\frac{1}{4})\theta}\,.$$

Let us move on to the case where the operator sits on a vertical edge, $e_0^{(x)}$:

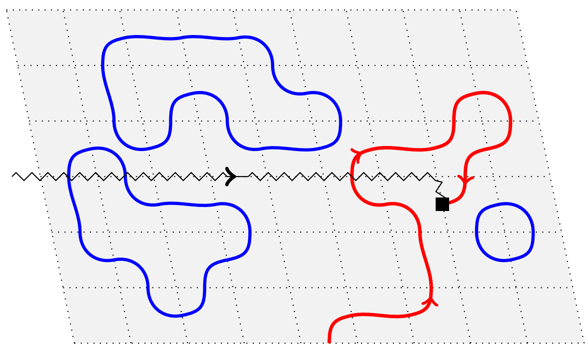

We now have $\theta = k\pi - \alpha$ with $k \in \mathbb{Z}$, and as in the previous case, the factor from the tail is $q^{2\lfloor k/2\rfloor}$. Putting everything together, we can again combine the two parities of k into a single summation

$$\left\langle e_0^{(x)}(x,t)\right\rangle = \frac{\varphi(q)z^{1-\ell}e^{i(\frac{\nu}{2}-\frac{1}{4})\alpha}}{Z} \sum_{C|\gamma:(x_d,1/2)\to(x,t)} W(C)\ e^{i(\frac{3\nu}{2}-\frac{1}{4})\theta}\,.$$

So far the value of ℓ (the constant introduced in the evaluation representation π_z) has been left arbitrary. In order to recover a discrete holomorphicity condition, we need the above formal expressions for $e_0^{(x)}$ and $e_0^{(t)}$ to differ by a factor of $e^{i\alpha}$, and hence we require that

$$w^{1-\ell} = \left[z^{1-\ell}e^{i(\nu/2-1/4)\alpha}\right] \times e^{i\alpha}\,. \tag{28}$$

Recalling that $(z/w)^{2\ell} = e^{-2i\nu\alpha}$, one can check (28) is satisfied by choosing $\ell = \frac{2\nu}{3(2\nu+1)}$. We now define

$$\phi_0(x,t) := \varphi(q)^{-1}w^{\ell-1}\begin{cases} e_0^{(t)}(x,t), & (x,t)\in(\mathbb{Z},\mathbb{Z}+\frac{1}{2}) \\ e^{i\alpha}e_0^{(x)}(x,t), & (x,t)\in(\mathbb{Z}+\frac{1}{2},\mathbb{Z}), \end{cases}$$

$$\langle\phi_0(x,t)\rangle = \frac{1}{Z}\sum_{C|\gamma:(x_d,1/2)\to(x,t)} W(C)\ e^{i(\frac{3\nu}{2}-\frac{1}{4})\theta}\,.$$

This observable satisfies the discrete holomorphicity condition:

$$\phi_0(x,t-1/2) + e^{i(\pi-\alpha)}\phi_0(x+1/2,t) - e^{i(\pi-\alpha)}\phi_0(x-1/2,t) - \phi_0(x,t+1/2) = 0\,. \tag{29}$$

As in the dense case, choosing $\bar{E}_0$ instead of E_0 would lead to the complex conjugate $\bar{\phi}_0$.

Remark: If one defines $\nu = \frac{1}{2} - \nu'$, then we get

$$\langle\phi_0(x,t)\rangle = \frac{1}{Z}\sum_{C|\gamma:(x_d,1/2)\to(x,t)} W(C)\ e^{-i(\frac{3\nu'}{2}-\frac{1}{2})\theta}\,,$$

and $x = z/w = e^{3i(\nu'-1)\alpha}$, which gives the same discretely holomorphic observable as in [18], but a different relationship between the ratio of spectral parameters x and the angle α.

4.2.2. *Loop observables associated to E_1 and $\bar{E}_1$.* The operator E_1 takes a spin $\downarrow$ to $\uparrow$. Hence, as in the dense model, we should consider two boundary defects, keeping the rest of the boundary empty for example. The insertion of operator E_1 at a given point then selects loop configurations such that the open path γ that starts/ends at the boundary defects passes through this point. Let us now compute explicitly the resulting factors. Firstly there is a factor of $w^{2\ell}$. For the winding of the γ from the boundary to the point in the bulk (and from the point in the bulk to the boundary), we obtain a total factor of $e^{-2i\nu\theta}$, where $\theta = k\pi$. Finally, for the crossings of the tail (which is now composed of T_1 matrices), we obtain a factor of $q^{4k} = e^{i(2\nu-1)\theta}$. Putting everything together, we have

$$\left\langle e_1^{(t)}(x,t)\right\rangle = \frac{w^{2\ell}}{Z} \sum_{C|(x,t)\in\gamma} W(C)\; e^{-i\theta}\,.$$

Notice that, in contrast to the dense case, here $e^{-i\theta}$ is not independent of the configuration since the parity of k is not fixed.

The calculation is completely analogous for $e_1^{(x)}$. Firstly there is a factor of $z^{2\ell}$. For the winding of γ we obtain a total factor of $e^{-2i\nu\theta}$, where $\theta = k\pi - \alpha$. Finally, for the crossings of the tail we obtain a factor of $q^{4k} = e^{i(2\nu-1)(\theta+\alpha)}$. Putting everything together gives

$$\left\langle e_1^{(x)}\right\rangle = \frac{z^{2\ell}e^{i(2\nu-1)\alpha}}{Z} \sum_{C|(x,t)\in\gamma} W(C)\; e^{-i\theta}\,.$$

Using $w^{2\ell} = z^{2\ell}e^{2i\nu\alpha}$, we define a function on the edges of the lattice

$$\phi_1(x,t) := w^{-2\ell}\begin{cases} e_1^{(t)}(x,t), & (x,t)\in\mathbb{Z}\times(\mathbb{Z}+\frac{1}{2})\\ e^{i\alpha}e_1^{(x)}(x,t), & (x,t)\in(\mathbb{Z}+\frac{1}{2})\times\mathbb{Z},\end{cases}$$

$$\langle\phi_1(x,t)\rangle = \frac{1}{Z}\sum_{C|(x,t)\in\gamma} W(C)\; e^{-i\theta}\,,$$

which satisfies the discrete holomorphicity condition

$$\phi_1(x,t-1/2) + e^{i(\pi-\alpha)}\phi_1(x+1/2,t) - e^{i(\pi-\alpha)}\phi_1(x-1/2,t) - \phi_1(x,t+1/2) = 0\,.$$

Again, using $\bar{E}_1$ we obtain the antiholomorphic counterpart $\bar{\phi}_1$.

5. Vertex models with integrable boundaries

5.1. **Coideal subalgebras and K-matrices.** Following the approach of [26], a left (resp. right) boundary quantized affine algebra B can be defined as a subalgebra of U with the left (resp. right) coideal property $\Delta : B \to B\otimes U$ (resp. $\Delta : B \to U\otimes B$). If V_z is irreducible as a B module, then the left (resp. right) boundary reflection matrix $K_\ell(z) : V_{z^{-1}} \to V_z$ (resp. $K_r(z) : V_z \to V_{z^{-1}}$) is the solution, unique up to an overall normalization, of the linear relation

$$K_\ell(z)\pi_{z^{-1}}(Y) = \pi_z(Y)K_\ell(z) \qquad \Big(\text{resp. } K_r(z)\pi_z(Y) = \pi_{z^{-1}}(Y)K_r(z)\Big) \tag{30}$$

for all $Y\in B$. We take the following as the graphical representation of $K_\ell(z)$ and $K_r(z)$:

$K_\ell(z) =$ 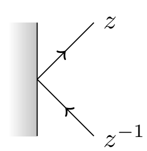

and $K_r(z) =$ 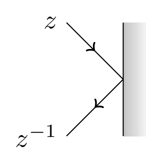

where we recall that the arrows represent the flow of time as one reads algebraic expressions from right to left.

From this, Sklyanin [26] defined a "double-row transfer matrix" $\mathbf{T}_2$:

$$\mathbf{T}_2(z; w_1, \ldots, w_L) = \mathrm{Tr}_0 \left(K_{\mathrm{r},0}(z) R_{0L}(z/w_L) \ldots R_{01}(z/w_1) K_{\mathrm{l},0}(z) R_{10}(zw_1) \ldots R_{L0}(zw_L) \right)$$

which has the graphical representation

$\mathbf{T}_2(z; w_1, \ldots, w_L) =$ 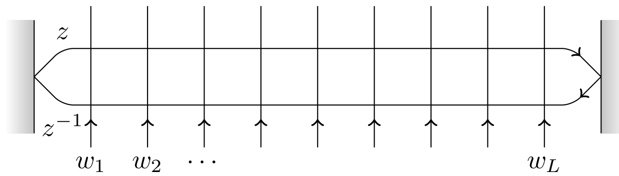

By vertically stacking M double-row transfer matrices $\mathbf{T}_2(z_i; w_1, \ldots, w_L)$, $1 \le i \le M$, one builds a rectangular lattice of width L and height $2M$, whose left/right boundary conditions are fixed *a priori.* Each $\mathbf{T}_2$ is an operator acting in $V_{w_1} \otimes \cdots \otimes V_{w_L}$.

5.2. **Current conservation at the boundary.** We now extend the formalism of [6] to the case of an integrable boundary. For simplicity, we treat only the case of the left boundary in full detail, but analogous relations can also be written for right boundaries.

Suppose we are given a left coideal subalgebra $B_\ell \subset U$, *i.e.*, a subalgebra with the additional property $\Delta(B_\ell) \subset B_\ell \otimes U$.[4] Assume also that we have a left boundary reflection matrix $K_\ell(z)$ which satisfies (30), for all $Y \in B_\ell$. Provided that $J_a \in B_\ell$, we have $K_\ell(z)\pi_{z^{-1}}(J_a) = \pi_z(J_a)K_\ell(z)$, which is represented graphically by

(31) 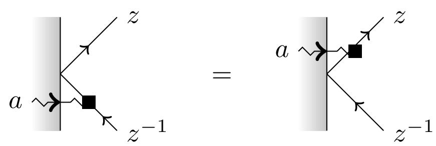

We have included tails of operators, but since with our conventions they extend to the left of the operator insertion, they never cross any lines and therefore play no role in equation (31). This equation expresses the local conservation of the current at the left boundary.

Similarly if ${\Theta_a}^b \in B_\ell$, we have $K_\ell(z)\pi_{z^{-1}}({\Theta_a}^b) = \pi_z({\Theta_a}^b)K_\ell(z)$, which has the graphical representation

(32) 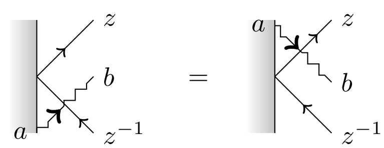

Analogous relations apply if J_a and ${\Theta_a}^b$ are elements of a right coideal subalgebra B_r with right boundary reflection matrix $K_r(z)$:

(33) 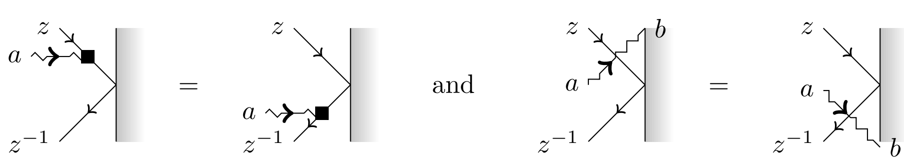

The result of the preceding equations is that we now obtain current and charge conservation laws which are *exact,* rather than correct up to boundary terms, as they were in § 2.3. For example, current conservation

[4]In view of the simple coproduct relations (3a–3b), one way to produce such a B_ℓ is to have it generated by appropriate combinations of the elements J_a and ${\Theta_a}^b$. We will discuss examples of such left coideal subalgebras in § 5.5.

(7) is now automatic, since the assumption that the tail commutes with the left boundary is implicit in the condition ${\Theta_a}^b \in B_\ell$.

Similarly, by using equations (5a) and (31)–(33), we find that

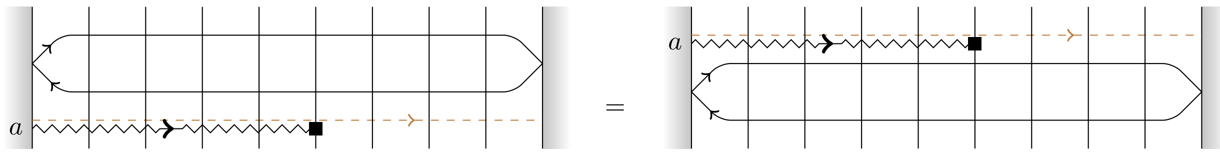

Graphically, this says that any charge built from $J_a, {\Theta_a}^b \in B_\ell, B_r$ commutes with the double-row transfer matrix; or equivalently, such a charge is conserved:

$$\mathbf{J}_a(t - 1/2) = \mathbf{J}_a(t + 3/2)\,. \tag{34}$$

5.3. **Light-cone lattice.** Let us now consider a specialization of the parameters w_i on the vertical lines in our lattice. We assume L to be even and choose

$$w_{j\ \mathrm{odd}} = z, \quad w_{j\ \mathrm{even}} = z^{-1}, \quad 1 \le j \le L.$$

Assuming that $R(1) \propto P$, which is the case for both $U = U_q(A_1^{(1)})$ and $U = U_q(A_2^{(2)})$, this causes every second R-matrix present in the lattice to degenerate into a P-matrix. The resulting "light-cone" lattice has half the number of vertices, with the remaining ones being rotated by 45 degrees. The double-row transfer matrix becomes

$\mathbf{T}_2 =$ 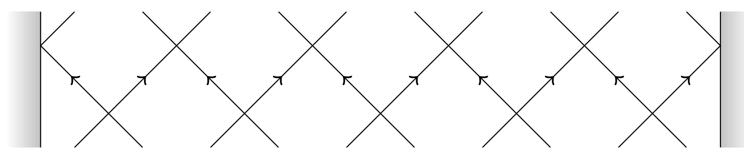

where we have absorbed an R-matrix in the right boundary; denote the resulting boundary operator $\tilde{K}_r(z)$ (we skip the details since we shall focus on the left boundary in what follows). All lines are now oriented upwards, so that we omit orientation arrows henceforth. Equivalently, $\mathbf{T}_2 = \mathbf{T}^e\mathbf{T}^o$, where

$\mathbf{T}_\mathrm{e} := K_\ell(z) \prod_i \check{R}_{2i}(z^2) \tilde{K}_r(z) =$ 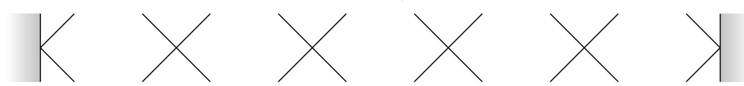

$\mathbf{T}_\mathrm{o} := \prod_i \check{R}_{2i+1}(z^2) =$ 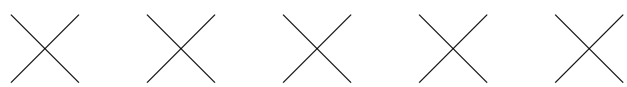

$\check{R}_i = P_{i,i+1} R_{i,i+1}$ is the R-matrix acting on sites $i, i+1$ with an additional permutation P of factors of the tensor product, and $K_\ell(z)$ (resp. $\tilde{K}_r(z)$) acts on the first (resp. last) factor of the tensor product.

Since the light-cone lattice is obtained as a special case of the double-row, two-boundary lattice, all previous results continue to apply; they only need to be transcribed into the new orientation. The analogue of relation (5a) is the commutation of $\check{R}$ with the action of J_a, that is:

(35) 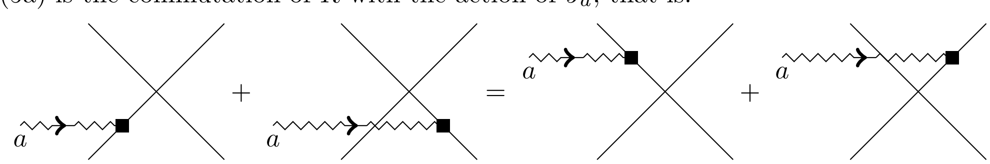

The 45 degree rotation makes "space" (resp. "time") lines go south-west to north-east (resp. south-east to north-west). The corresponding currents are simply

$j_a(x) =$ 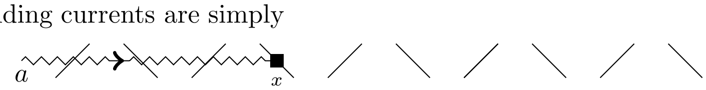

(or opposite tilt of the lines depending on parity of t), where $x \in \mathbb{Z}$ and the former distinction between "time" and "space" components is uneccessary. The same conservation equation (7) holds as a consequence of (35), and the fact that ${\Theta_a}^b \in B_\ell$. Rewritten in the light-cone approach, it becomes:

$$j_a(x,t) + j_a(x+1,t) = j_a(x,t+1) + j_a(x+1,t+1)\,, \qquad (x,t) \in \mathbb{Z}^2,\ x+t=0 \pmod 2\,. \tag{36}$$

Similarly, (31) can be rewritten algebraically as

$$j_a(1,t) = j_a(1,t+1)\,, \qquad t = 0 \pmod 2\,. \tag{37}$$

There is a right boundary analogue:

$$j_a(L,t) = j_a(L,t+1)\,, \qquad t = 0 \pmod 2\,. \tag{38}$$

The charge $\mathbf{J}_a$ is now the obvious sum: $\mathbf{J}_a = \sum_{x=1}^{L} j_a(x)$, or graphically,

(39) $\mathbf{J}_a =$ 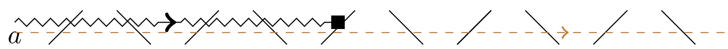

and as a direct consequence of (36–38), commutes with both $\mathbf{T}_\mathrm{e}$ and $\mathbf{T}_\mathrm{o}$, *i.e.*,

$$\mathbf{J}_a(t) = \mathbf{J}_a(t+1)\,. \tag{40}$$

As already pointed out, we are mainly concerned with local current conservation rather than conservation of the charge; in particular the local conservation at the left boundary (37) only requires integrability at the left boundary.

5.4. **Adjoint action on the light-cone lattice.** The adjoint action of an element J_a of U on another element J_b is defined as in (9). On the light-cone lattice, and in the case of an operator J_a commuting with K-matrices on all boundaries, the expression of $A_a[j_b^{(t)}]$ can be greatly simplified. We illustrate this by a series of pictures in which, in preparation for the switch to loop models, we use dual lattice pictures, *cf.* (16) in the bulk, and at the boundary, $K_\ell =$ 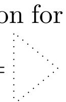 and similarly for the other boundaries.

Using the conservation equation (40), the contour defining $A_a[j_b^{(t)}]$ can be deformed to follow the top and bottom boundaries, *i.e.*,

$A_a[j_b(x,t)] =$ 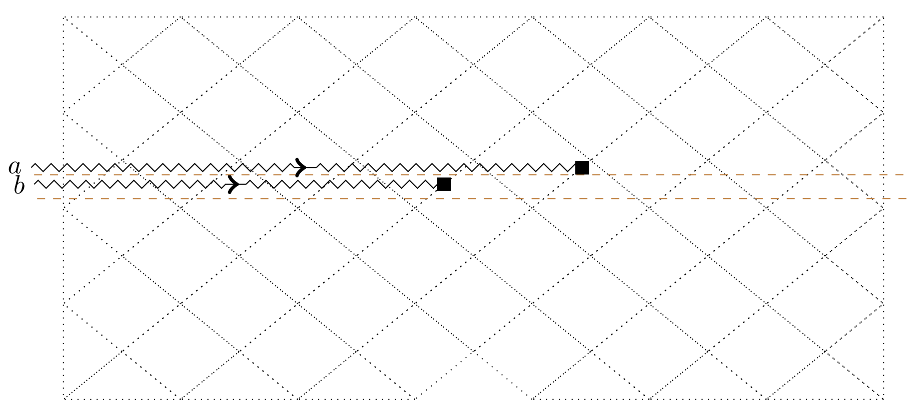

$=$

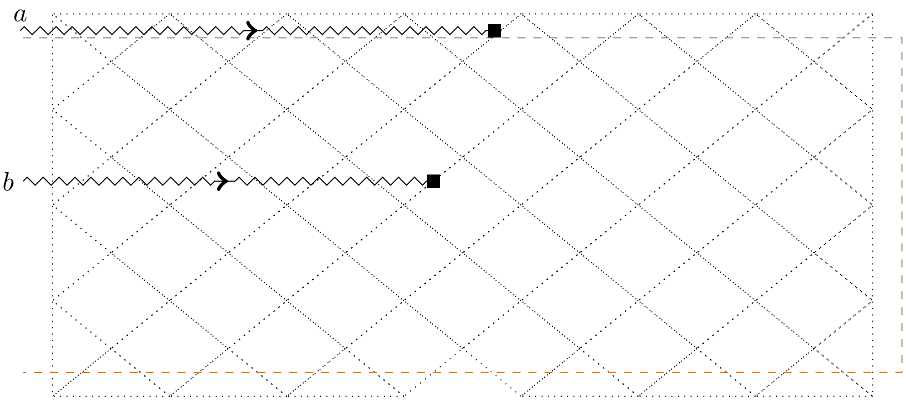

We now suppose that top and bottom boundary conditions are also integrable, such that J_a commutes with the corresponding K-matrices, except at some boundary defects which sit say on the bottom boundary. Then the top part of the contour can be moved through the top row of K-matrices, using again the boundary conservation relations. Indeed, the sum over the two points on each triangle along the top boundary gives a zero contribution.[5] On the bottom part, the contour is reduced to an arch enclosing the defects:

$A_a[j_b(x,t)] =$

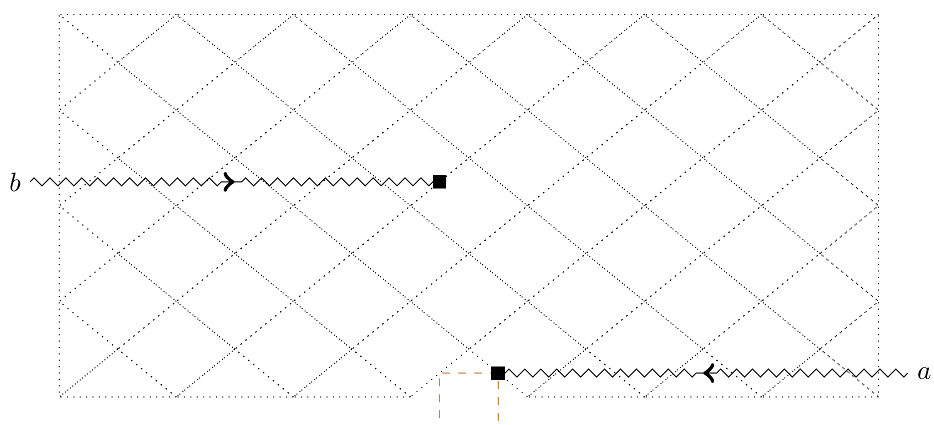

Translating this final picture into algebraic form, we obtain

$$\langle A_a[j_b(x,t)]\rangle = \langle [\widehat{\jmath}_a(x_d,0) + \widehat{\jmath}_a(x_d+1,0)]\, j_b(x,t)\rangle \ , \tag{41}$$

where we assume that there are two defects at adjacent locations x_d and x_d+1, and recalling that $\widehat{\jmath}_a$ denotes a non-local current with a "right" tail, *cf.* § 2.2.

5.5. **Coideal subalgebras for quantized affine algebras.** Here we give examples of (left) coideal subalgebras and boundary reflection matrices for the quantized affine algebras that interest us. Since we do not discuss analogous right boundary results, we omit the subscript "ℓ" from all subsequent equations.

5.5.1. *The $U_q(A_1^{(1)})$ boundary algebra.* The choice of coideal subalgebra B we shall consider in this paper is generated by

$$\{T_0\,, T_1\,, Q := E_1 + r\bar{E}_0\,, \bar{Q} := \bar{E}_1 + rE_0\}\,,$$

[5] To see this, we must pay attention to a crucial sign issue – our currents are associated to edges which are oriented upwards, so current conservation at the top/bottom boundaries must be accompanied by a sign in one of the terms. It is precisely this sign which causes the pairwise cancellation for each triangle.

where r is a real parameter. The left coideal property is satisfied because

$$\Delta(Q) = Q \otimes 1 + T_1 \otimes E_1 + T_0 \otimes r\bar{E}_0 \qquad \text{and} \qquad \Delta(\bar{Q}) = \bar{Q} \otimes 1 + T_1 \otimes \bar{E}_1 + T_0 \otimes rE_0$$

are both elements of $B \otimes U$. After a choice of normalization the solution of (30) is [21]

$$K(z) = \begin{pmatrix} z + rz^{-1} & 0 \\ 0 & z^{-1} + rz \end{pmatrix} . \tag{42}$$

Note that $K(z)$ is diagonal as a consequence of the fact that T_0 and T_1 are elements of B.

5.5.2. *The $U_q(A_2^{(2)})$ boundary algebra.* The boundary algebra B in this case is taken to be that generated by $\{T_0, T_1, E_1, \bar{E}_1, Q, \bar{Q}\}$, where

$$Q := [E_1, E_0]_{q^{-4}} + r\bar{E}_0\,, \qquad \bar{Q} := [\bar{E}_1, \bar{E}_0]_{q^4} - rq^2 E_0\,.$$

in which we use the notation $[a, b]_x = ab - xba$.

The left coideal property $\Delta(B) \in B \otimes U$ is easy to check. With a choice of normalization, the solution of (30) in the case when r is fixed to be $r = \pm iq^{-1}$ reads [2, 22]

$$K(z) = \begin{pmatrix} z^{2\ell}(z^{-1} + rz) & 0 & 0 \\ 0 & z + rz^{-1} & 0 \\ 0 & 0 & z^{-2\ell}(z^{-1} + rz) \end{pmatrix} . \tag{43}$$

For definiteness, we shall henceforth take the root $r = iq^{-1}$. As in the $U_q(A_1^{(1)})$ model case , $K(z)$ is diagonal because T_0 and T_1 are elements of B. In contrast to the $U_q(A_1^{(1)})$ case, there is no solution of (30) for general values of the parameter r.

6. Integrable boundaries for loop models

In this section we repeat the ideas of § 3 to introduce boundary tiles into the dense and dilute Temperley–Lieb models. In complete analogy with § 3, the corresponding K matrices (42) and (43) are recovered as linear combinations of the boundary tiles. We use the light-cone approach of § 5.3, with an angle of α on the lattice, *i.e.*,

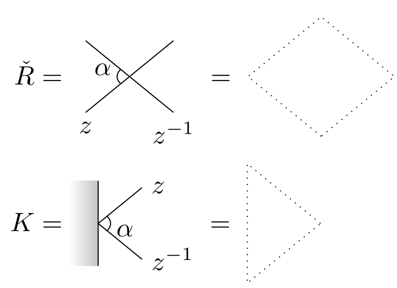

and similarly for other boundaries.

6.1. **The boundary dense Temperley–Lieb model and the $U_q(A_1^{(1)})$ vertex model.** Let us define a boundary loop model by introducing an additional weight 1 boundary plaquette, as follows:

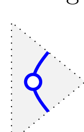
,

and by assigning weight $\tau^{(n)} = -(e^{i\nu(2\pi-n\xi)} + e^{-i\nu(2\pi-n\xi)})$ to any loop that that passes n times through a boundary. Thus we can view the boundary as introducing a deficit angle of ξ.

Again, we can turn this boundary weight into that of a vertex model by viewing it as an operator from $V \to V$ in a S-N direction, resulting in a boundary weight

$$K = \begin{pmatrix} e^{-i\nu(\alpha-\xi)} & 0 \\ 0 & e^{i\nu(\alpha-\xi)} \end{pmatrix}. \tag{44}$$

Since the spectral parameter z is related to the angle α by $z = e^{-i\nu\alpha}$, this boundary matrix coincides with $K(z)$ of (42)[6] if we take

$$e^{2i\nu\xi} = (1 + rz^{-2})/(1 + rz^2).$$

Clearly the $r = 0$ case corresponds to a zero deficit angle $\xi = 0$ in which case the boundary TL plaquette becomes the single plaquette with weight one which we call “free boundary conditions” and denote by

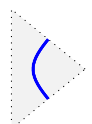

6.2. **The boundary dilute Temperley–Lieb model and the $U_q(A_2^{(2)})$ vertex model.** We introduce two additional boundary plaquette configurations with associated weights ρ and κ, as follows:

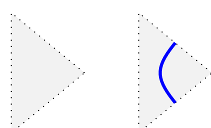

ρ κ

Interpreting the plaquettes as operators as above yields a boundary reflection matrix

$$K = \begin{pmatrix} \kappa e^{-i\nu\alpha} & 0 & 0 \\ 0 & \rho & 0 \\ 0 & 0 & \kappa e^{i\nu\alpha} \end{pmatrix}, \tag{45}$$

which is equal to the matrix $K(z)$ of equation (43) if $\rho = z + iq^{-1}z^{-1}$ and $\kappa = z^{-1} + iq^{-1}z$, using also the fact that $z^{2\ell} = e^{-i\nu\alpha}$.

7. Non-local currents and boundary discrete holomorphicity

7.1. **Application to the dense loop model.** For convenience, in this section we shall use exclusively the light-cone orientation of the lattice. We consider loop configurations on the lattice which contain a single open path γ. For simplicity, we assume that the ends of γ are situated next to each other, as follows:

[6] In fact the two K-matrices coincide after renormalizing (44) by $((1 + rz^{-2})(1 + rz^2))^{1/2}$. Since this only produces a global factor in the observables we will consider, we omit this normalization for simplicity.

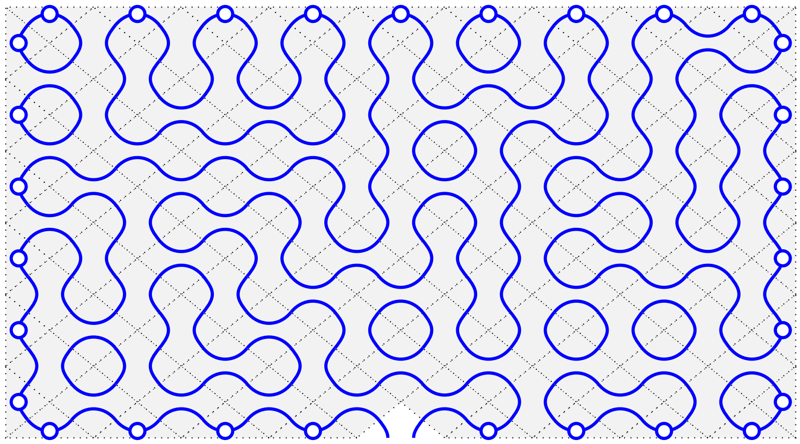

As we did in the case of trivial boundary conditions, we consider observables which are constructed by requiring that the open loop goes through a certain point (x, t), either in the bulk or on the boundary of the lattice. Because the K-matrices are diagonal the correct way to obtain such observables is, as before, to insert a local operator (say E_0, complete with its tail) at (x, t), since all lattice configurations vanish for which E_0 is situated on a closed loop:

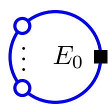

$$= 0\,.$$

7.1.1. *Loop observables in the bulk.* Let us repeat the analysis of the observables in the bulk, but now in the presence of non-trivial boundaries and on the light-cone lattice. Insert e_0 at the point $(x+1, t) \in \mathbb{Z}^2$, $x + t = 0 \pmod 2$, in the bulk of the lattice. As mentioned above, the only configurations which survive are those for which the open loop goes through $(x + 1, t)$. The contribution of the open path to the weight can be found in a similar way as before as $e^{i\nu(2\theta-\pi+n\xi)}q^k$, where $\theta = k\pi$ is the angle formed by the left-incoming portion of the open loop (if we treat the boundary tiles on equal footing with bulk tiles), and n the number of contacts of the left portion of this loop with the boundary minus that of the right portion. So we find

$$\langle e_0(x+1,t)\rangle = \frac{z^{-1}e^{-i\nu\pi}}{Z} \sum_{C|(x+1,t)\in\gamma} W(C)\; e^{i(4\nu-1)\theta}\; e^{ni\nu\xi}\,,$$

Similarly, repeating for $e_0(x, t)$ with $x + t = 0 \pmod 2$, we obtain

$$\langle e_0(x,t)\rangle = \frac{z\,e^{-i\nu\pi}e^{i(2\nu-1)\alpha}}{Z} \sum_{C|(x,t)\in\gamma} W(C)\; e^{i(4\nu-1)\theta}e^{ni\nu\xi}\,.$$

The local conservation law (36) with $j_a = e_0$ is

$$e_0(x,t) + e_0(x+1,t) = e_0(x,t+1) + e_0(x+1,t+1)\,, \qquad (x,t)\in\mathbb{Z}^2,\ x+t=0 \pmod 2\,. \tag{46}$$

This holds in the bulk because the tail, which is comprised of T_0 operators, commutes with the left K-matrix (since $T_0 \in B$, as explained in § 5.5.1). Therefore, using analogous arguments to those of § 4.1, we define the function

$$\phi_0(x,t) := ze^{i\nu\pi}\begin{cases} e_0(x,t), & x+t=1 \pmod 2 \\ e^{i\alpha}e_0(x,t), & x+t=0 \pmod 2\,, \end{cases}$$

and in view of the fact that $z = e^{-i\nu\alpha}$, we have

$$\langle \phi_0(x,t) \rangle = \frac{1}{Z} \sum_{C | (x,t) \in \gamma} W(C)\ e^{i(4\nu-1)\theta} e^{ni\nu\xi}\,. \tag{47}$$

Applying (46) to this observable, we find that it satisfies

$$e^{i(\pi-\alpha)}\phi_0(x,t) + \phi_0(x+1,t) - e^{i(\pi-\alpha)}\phi_0(x+1,t+1) - \phi_0(x,t+1) = 0\,,$$

which is discrete holomorphicity on the light-cone lattice.

The observable corresponding to insertion of E_1 gets modified in an analogous way; namely

$$\phi_1(x,t) := z e^{-i\nu\pi} \begin{cases} e_1(x,t), & x+t = 1 \pmod 2 \\ e^{i\alpha} e_1(x,t), & x+t = 0 \pmod 2 \end{cases}$$

gives rise to the observable

$$\langle \phi_1(x,t) \rangle = \frac{1}{Z} \sum_{C | (x,t) \in \gamma} W(C)\ e^{-i\theta}\ e^{-ni\nu\xi}\,. \tag{48}$$

This is the flux observable in the presence of a non-trivial boundary and it satisfies the discrete holomorphicity equation

$$e^{i(\pi-\alpha)}\phi_1(x,t) + \phi_1(x+1,t) - e^{i(\pi-\alpha)}\phi_1(x+1,t+1) - \phi_1(x,t+1) = 0\,.$$

7.1.2. *Loop observables at the boundary.* By *boundary* we mean in what follows the *left* boundary. Since $r \neq 0$, the operators $E_0, E_1, \bar{E}_0, \bar{E}_1$ are not elements of the coideal B, and hence they are not conserved separately at the boundary (with trivial boundaries, E_1 and $\bar{E}_1$ were conserved), and in particular their associated charge will not be conserved.

We now consider the combinations $Q = E_1 + r\bar{E}_0$ and $\bar{Q} = \bar{E}_1 + rE_0$, which are in B. Using (37) in the case $j_a = e_1 + r\bar{e}_0$ we find that

$$e_1(1,t) + r\bar{e}_0(1,t) = e_1(1,t+1) + r\bar{e}_0(1,t+1)\,, \qquad t = 0 \pmod 2\,,$$

which can be translated into the following equation for the observables ϕ_1 and $\bar{\phi}_0$:

$$z^{-1}\phi_1(1,t) + rz\bar{\phi}_0(1,t) = e^{-i\alpha} z^{-1}\phi_1(1,t+1) + e^{i\alpha} rz\bar{\phi}_0(1,t+1)\,.$$

This is neither a holomorphicity nor an antiholomorphicity condition because we are mixing operators from the two chiralities. However, by taking the real part (or equivalently, summing this identity and the one satisfied by the conjugate observable $\bar{Q}$), one finds that $\psi := z^{-1}(\phi_1 + r\phi_0)$ satisfies

$$\mathrm{Re}\left[\psi(1,t) + e^{i(\pi-\alpha)}\psi(1,t+1)\right] = 0\,,$$

which is a boundary discrete holomorphicity condition around the plaquette

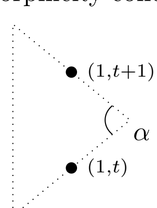

$t = 0 \pmod 2$.

Remark: At the left boundary the tails (which are on the left) disappear and therefore the two observables ϕ_1 and $\bar{\phi}_0$ are the same up to a constant. This can be seen more explicitly in the fact that there cannot be any winding at the boundary, so the angle θ in (47,48) is fixed and independent of the configuration.

7.2. **Application to the dilute loop model.** We consider the dilute loop model on the light-cone lattice, with as in the dense case possible defects located next to each other on the bottom row. All the observables that we consider force a line to go from the insertion point to the boundary defect, so that a typical configuration is as depicted below.

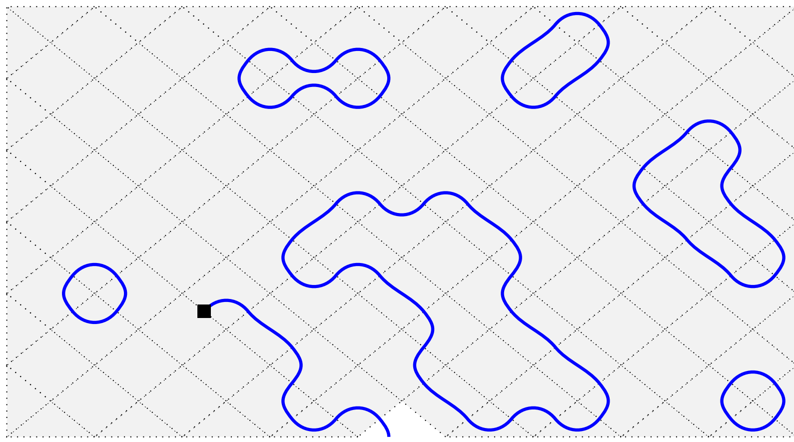

7.2.1. *Loop observables in the bulk.* In contrast with the dense case, the K-matrix (43) does not introduce any orientation-dependent phase factor, but simply a relative weight for contacts with the boundary. Therefore, the analysis of observables E_0 and E_1 in the bulk is unchanged, and we do not repeat it here.

A natural question is whether one can use the adjoint action to build new currents. We consider the element $P \in U_q(A_2^{(2)})$ given by $P = \mathrm{ad}_{E_1}(E_0)$. Explicitly,

$$P = E_1 E_0 - T_1 E_0 T_1^{-1} E_1 = E_1 E_0 - q^{-4} E_0 E_1 \,,$$

and hence we can use the treatment of § 5.4 to express the corresponding lattice observable p. From (41), we have

$$\langle p(x,t)\rangle = \langle A_{E_1}[e_0(x,t)]\rangle = \langle [\widehat{e}_1(x_d,0) + \widehat{e}_1(x_d+1,0)]\, e_0(x,t)\rangle \ .$$

Since E_1 can only flip a state $\downarrow$ to a state $\uparrow$, the non-zero terms correspond to a pair of defects $(\downarrow, 0)$ or $(0, \downarrow)$. Summing over these two possibilities, we get: $\langle p(x,t)\rangle = -q^{-4}(z^{2\ell} + z^{-2\ell})\,\langle e_0(x,t)\rangle$. Hence, the operator P does not lead to a new holomorphic observable; it simply produces ϕ_0, up to a multiplicative constant.

Equivalently, let us define

$$\xi(x,t) := z^{\ell-1}\begin{cases} p(x,t), & x+t=1 \pmod 2 \\ e^{i\alpha}p(x,t), & x+t=0 \pmod 2\,, \end{cases} \qquad \phi_0(x,t) := z^{\ell-1}\begin{cases} e_0(x,t), & x+t=1 \pmod 2 \\ e^{i\alpha}e_0(x,t), & x+t=0 \pmod 2\,. \end{cases}$$

Then

$$\langle \xi(x,t)\rangle = c\,\langle \phi_0(x,t)\rangle\,, \qquad \text{where} \ \ c = -q^{-4}(z^{2\ell} + z^{-2\ell}). \tag{49}$$

Since it is only possible to relate ξ and ϕ_0 as expectation values $\langle\cdots\rangle$, the constant c is dependent on the choice of boundary conditions; it would differ, had we chosen alternative boundaries to the ones shown in the figure above.

7.2.2. *Loop observables at the boundary.* We are now in a position to construct an observable which satisfies discrete holomorphicity at the left boundary. We consider the operator $Q = P + iq^{-1}\bar{E}_0$ (with P as in the previous section), which commutes with the K-matrix in the sense of (30), *cf.* §5.5.2.

From (37) with $j_a = p + iq^{-1}\bar{e}_0$ we obtain

$$p(1,t) + iq^{-1}\bar{e}_0(1,t) = p(1,t+1) + iq^{-1}\bar{e}_0(1,t+1)\,,$$

which can be translated into an equation for the observables ξ and $\bar{\phi}_0$:

$$z^{1-\ell}\xi(1,t) + iq^{-1}z^{\ell-1}\bar{\phi}_0(1,t) = e^{-i\alpha}z^{1-\ell}\xi(1,t+1) + e^{i\alpha}iq^{-1}z^{\ell-1}\bar{\phi}_0(1,t+1)\,.$$

Taking the real part of this equation, we obtain

$$\mathrm{Re}\left[\psi(1,t) + e^{i(\pi-\alpha)}\psi(1,t+1)\right] = 0\,,$$

where $\psi = z^{1-\ell}(\xi - iq\phi_0)$. Now taking into account (49), we find that in the equation above one can replace ψ with $e^{i\lambda}\phi_0$ (λ being some phase, dependent on our choice of boundary conditions, which we do not write explicitly).

8. The continuum limit

8.1. **Dense loops.** In this section, we identify the operators corresponding to the lattice holomorphic observables, as holomorphic currents in the CFT describing the continuum limit.

8.1.1. *Scaling theory.* Let us first briefly review the Coulomb gas construction [23, 12]. We define a height function $\Phi(x+1/2, t+1/2)$ on the dual lattice, such that the oriented loops are the contour lines of Φ, and with the convention that the values of Φ across a contour line differ by π. In the continuum limit, the height function is then subject to a Gaussian distribution:

$$S[\Phi] = \frac{g}{4\pi}\int (\nabla\Phi)^2 dx dt\,, \qquad \text{where} \qquad g = 1 - 2\nu\,. \tag{50}$$

Note that the coupling constant spans the interval $0 < g < 1$. In what follows, the model is defined on a cylinder of even circumference L, and the axis of the cylinder is in the time direction. Because of the definition of Φ by local increments, Φ can be discontinuous along the circumference:

$$\Phi(L + x + 1/2, t + 1/2) - \Phi(x + 1/2, t + 1/2) = 2\pi m\,, \qquad m \in \mathbb{Z}\,.$$

Thus, the height function should be considered as living on a circle:

$$\Phi \equiv \Phi + 2\pi\,.$$

Also, the local Boltzmann weights associated to loop turns ensure that the closed loops get the correct weight $\tau = 2\cos(2\pi\nu)$, except for the non-contractible loops: these loops have a vanishing total winding, and thus get a weight $\widetilde{\tau} = 2$. To restore the correct weight, one introduces a seam in the time direction, such that every right (resp. left) arrow crossing the seam gets a weight $e^{i\pi\alpha}$ (resp. $e^{-i\pi\alpha}$). The weight of non-contractible loops becomes $\widetilde{\tau} = 2\cos\pi\alpha$, and one sets $\alpha := 2\nu$ to get $\widetilde{\tau} = \tau$.

8.1.2. *Operator content.* To recover the full-plane geometry, we use the complex coordinates

$$z = e^{2\pi(t+ix)/L}\,, \qquad \bar{z} = e^{2\pi(t-ix)/L}\,.$$

In this setting, the seam described above goes from the origin to infinity, and amounts to introducing a pair of vertex operators $e^{i\alpha\Phi(\infty)}e^{-i\alpha\Phi(0)}$. More generally, if we decompose the height field as $\Phi(z,\bar{z}) = \varphi(z) + \bar{\varphi}(\bar{z})$, the primary operators are of the form $\mathcal{O}_{\mu,\bar{\mu}} = e^{i(\mu\varphi + \bar{\mu}\bar{\varphi})}$, which we write as

$$\mathcal{O}_{\mu,\bar{\mu}} = e^{i(\mu+\bar{\mu})(\varphi+\bar{\varphi})/2} \times e^{i(\mu-\bar{\mu})(\varphi-\bar{\varphi})/2}\,.$$

The first factor is only well-defined if $n := (\mu + \bar{\mu})/2$ is an integer, which is called the electric charge. The average value of the second factor is $e^{i\Phi_{\mathrm{cl}}}$, where $\Phi_{\mathrm{cl}} = i(\mu - \bar{\mu})(\log z - \log\bar{z})/(4g)$. The discontinuity of Φ_{cl} around the origin is $\delta\Phi_{\mathrm{cl}} = 2\pi \times (\mu - \bar{\mu})/(2g)$, and hence the number $m := (\mu - \bar{\mu})/(2g)$ must be an integer, which is called the magnetic charge. Since the conformal weight of the chiral vertex operator $e^{i\mu\varphi}$ is $h_\mu = \mu(\mu+2\alpha)/(4g)$, we get for $\mathcal{O}_{\mu,\bar\mu}$:

$$h = \frac{(n+\alpha+mg)^2-\alpha^2}{4g}\,, \qquad \bar h = \frac{(n+\alpha-mg)^2-\alpha^2}{4g}\,,$$

with $n,m\in\mathbb{Z}^2$. In this context, α appears as a background electric charge. Part of the above spectrum fits in the Kac table for minimal models:

$$h_{r,s} = \frac{(r-gs)^2-(1-g)^2}{4g}\,,$$

with integer r,s.

8.1.3. *Scaling limit of the lattice observables.* We will now show that the discrete (anti-)holomorphic observables discussed in this paper scale to operators of the form $\mathcal{O}_{\mu,\bar\mu}$. Let us first consider the two-point function associated to E_0:

$$\langle \phi_0(z,\bar z)\phi_0^*(w,\bar w)\rangle := \frac{1}{Z}\sum_{C|\gamma_1,\gamma_2:w\to z} e^{i(4\nu-1)\theta}\ W(C)\,,$$

where the sum is on loop configurations with two open oriented paths γ_1,γ_2 going from w to z, and θ is the winding angle of each path. In terms of the height model, this correlation function includes magnetic defects of charges -1 and $+1$ at z and w, respectively. Moreover, the winding angle is given by $\theta=\Phi(z,\bar z)-\Phi(w,\bar w)$, and hence the factor $e^{i(4\nu-1)\theta}$ corresponds to an electric operator of charge $n+\alpha=4\nu-1$ at z, and opposite charge at w. These charges yield the values $\mu=-2g$ and $\bar\mu=0$, and thus we identify:

$$\phi_0 = \phi_0(z) = e^{-2ig\varphi(z)}\,,$$

with conformal dimensions $h=2g-1=h_{13}$ and $\bar h=0$. By reversing the arrows, we obtain

$$\bar\phi_0(\bar z) = e^{-2ig\bar\varphi(\bar z)}\,.$$

Similarly, the two-point function associated to E_1 is:

$$\langle \phi_1(z,\bar z)\phi_1^*(w,\bar w)\rangle := \frac{1}{Z}\sum_{C|\gamma_1,\gamma_2:w\to z} e^{i\theta}\ W(C)\,,$$

which has charges $m=1$ and $n+\alpha=1$, and hence we get

$$\phi_1(z) = e^{2ig\varphi(z)}\,, \qquad \bar\phi_1(\bar z) = e^{2ig\bar\varphi(\bar z)}\,.$$

The holomorphic current ϕ_1 has conformal dimensions $h=1$ and $\bar h=0$: this is the "screening operator".

We now turn to the lattice operator associated to the diagonal generators H_i. Since $H_i\propto\sigma^z$, it simply measures the local orientation of loops. The increment of Φ across an up (resp. down) arrow is π (resp. $-\pi$), and thus one has $a\partial_x\Phi=\pi h^{(t)}$, and likewise $a\partial_t\Phi=-\pi h^{(x)}$, where a is the lattice mesh size. Using the complex coordinates $w=t+ix$ and $\bar w=t-ix$, we identify the chiral currents:

$$h^{(x)}+ih^{(t)}\propto\partial_w\varphi\,, \qquad h^{(x)}-ih^{(t)}\propto\partial_{\bar w}\bar\varphi\,,$$

The conservation law found in § 4.1.3 corresponds in the continuum limit to the conservation of non-chiral current $d^*\Phi=d^*(\varphi+\bar\varphi)$, or in components, $\epsilon^{\mu\nu}\partial_\nu\Phi$, which ensures local well-definedness of Φ.

The above results can be summarised in the following diagram:

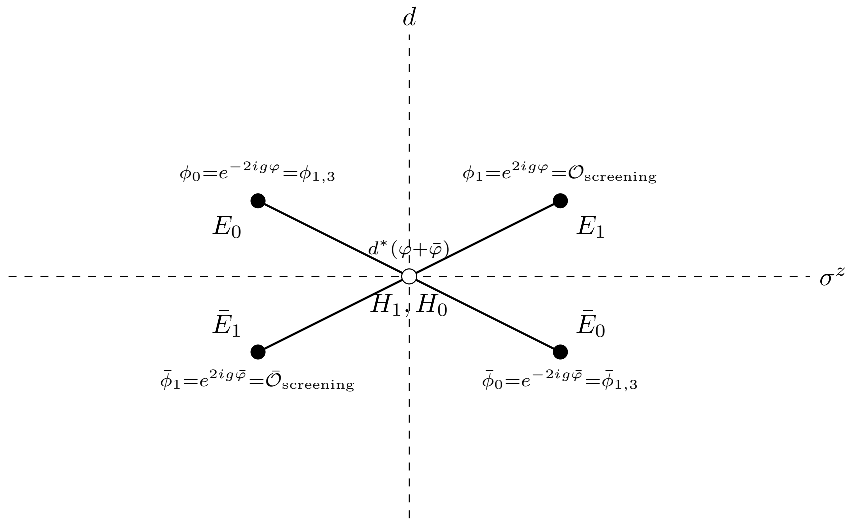

In this figure, the horizontal axis is the $U(1)$ charge σ^z, and the vertical axis is the gradation d in the evaluation representation of $A_1^{(1)}$. We note the similarity with the discussion of nonlocal charges in the (ultra-violet limit of the) sine–Gordon model in [7]. A notable difference is the choice of gradation, which has different origins in the two situations.

8.2. **Dilute loops.** The mapping to a compactified free boson CFT (50) also holds in the dilute case, up to minor adaptations. We keep the convention that the height function Φ has jumps of $\pm\pi$ across an oriented loop. Since empty edges are now allowed, this means that the discontinuities of Φ along the circumference of the cylinder are now multiples of π, and one should set $\Phi \equiv \Phi + \pi$. So we can keep the same notations as in the previous section, except that the allowed electromagnetic charges become: $m \in \mathbb{Z}/2$ and $n \in 2\mathbb{Z}$. Moreover, ν is now chosen in the interval $[-1/2, 0]$, and we have $1 < g < 2$.

The two-point function for ϕ_0 is:

$$\langle \phi_0(z,\bar z)\phi_0^*(w,\bar w)\rangle = \frac{1}{Z}\sum_{C|\gamma:w\to z} e^{i(3\nu/2-1/4)\theta}\ W(C)\,,$$

where the sum is on loop configurations with one open oriented path γ going from w to z, and θ is the winding angle of γ. Since this is a one-leg defect and $\theta = 2[\Phi(z,\bar z) - \Phi(w,\bar w)]$, the corresponding charges are $m = -1/2$ and $n + \alpha = 3\nu - 1/2$. The "flux observables" ϕ_1 and $\bar\phi_1$ are the same as in the dense model. Thus we obtain

$$\phi_0(z) = e^{-ig\varphi(z)}\,, \qquad \bar\phi_0(\bar z) = e^{-ig\bar\varphi(\bar z)}\,,$$
$$\phi_1(z) = e^{2ig\varphi(z)}\,, \qquad \bar\phi_1(\bar z) = e^{2ig\bar\varphi(\bar z)}\,,$$

and the conformal dimension for ϕ_0 is $h = (3g-2)/4 = h_{12}$, whereas for ϕ_1 it is $h = 1$. Finally, the diagonal operators $h^{(x,t)}$ relate to $\partial_w\varphi$ and $\partial_{\bar w}\bar\varphi$.

9. Conclusions

In this paper, we have described a general procedure to obtain discretely holomorphic observables out of nonlocal currents in quantum integrable lattice models. We have shown in several examples how these observables are naturally expressed in terms of loop models. We have identified them in the continuum limit, connecting to Conformal Field Theory.

It should be noted that in CFT the conserved currents always come in pairs: a current j^μ and its dual current $\tilde{\jmath}^\mu = \epsilon^\mu_\nu j^\nu$. Only the two conservation laws combined imply separation of chiralities, and therefore existence of holomorphic observables. Here we only base our analysis on a single conservation law for each observable, hence a "weak" discrete holomorphicity condition – the dual equation is missing. This absence can be traced to the step in which we identify the two components (say, time and space) of our current as a single function corresponding to the observable. This step would require additional justification in order to proceed with a rigorous proof of the conformal limit.[7] The fact that in all cases, our would-be chiral observables have, in the loop language, a unifying definition on both vertical and horizontal edges is certainly a strong indication that such an identification is correct.

This work opens the way to further study and interpretation of discrete holomorphic observables, in particular in the case of more general boundary conditions (as recently studied in [11]). Also, the application of this approach to off-critical models (see the treatment of the Ising model in [25]) needs to be developed.

References

[1] I. Alam and M. Batchelor, *Integrability as a consequence of discrete holomorphicity: the $\mathbb{Z}_N$ model*, 2012, preprint, `arXiv:1207.3883`.

[2] M. T. Batchelor, V. Fridkin, A. Kuniba, and Y. K. Zhou, *Solutions of the reflection equation for face and vertex models associated with $A_n^{(1)}, B_n^{(1)}, C_n^{(1)}, D_n^{(1)}$ and $A_n^{(2)}$*, Physics Letters B **376** (1996), no. 4, 266 – 274.

[3] R. J. Baxter, *Exactly solved models in statistical mechanics*, second ed., Dover, USA, 2007, Reprint of the 1982 original (Academic Press, London).

[4] N. Beaton, J. de Gier, and A. Guttmann, *The critical fugacity for surface adsorption of SAW on the honeycomb lattice is* $1+\sqrt{2}$, September 2011, preprint, `arXiv:1109.0358`.

[5] N. Beaton, A. Guttmann, and I. Jensen, *Two-dimensional self-avoiding walks and polymer adsorption: critical fugacity estimates*, J. Phys. A **45** (2012), no. 5, 055208, `http://stacks.iop.org/1751-8121/45/i=5/a=055208`.

[6] D. Bernard and G. Felder, *Quantum group symmetries in two-dimensional lattice quantum field theory*, Nucl. Phys. B **365** (1991), no. 1, 98 – 120, `doi`.

[7] D. Bernard and A. Leclair, *Quantum group symmetries and non-local currents in 2d QFT*, Commun. Math. Phys. **142** (1991), 99–138 (English), `doi`.

[8] V. Chari and A. Pressley, *A guide to quantum groups*, Cambridge, 1994.

[9] D. Chelkak, C. Hongler, and K. Izyurov, *Conformal invariance of spin correlations in the planar Ising model*, February 2012, preprint, `arXiv:1202.2838`.

[10] D. Chelkak and S. Smirnov, *Universality in the 2D Ising model and conformal invariance of fermionic observables*, October 2009, preprint, `arXiv:0910.2045`.

[11] J. de Gier, A. Lee, and J. Rasmussen, *Discrete holomorphicity and integrability in loop models with open boundaries*, October 2012, preprint, `arXiv:1210.5036`.

[12] P. Di Francesco, H. Saleur, and J.-B. Zuber, *Relations between the Coulomb gas picture and conformal invariance of two-dimensional critical models*, J. Stat. Phys. **49** (1987), 57–79, `doi`.

[13] Vl. Dotsenko and A. Polyakov, *Fermion representations for the 2d and 3d Ising models*, Adv. Stud. Pure Math. **16** (1988), 171–203, Conformal field theory and solvable lattice models, Ed. by M. Jimbo, T. Miwa, A. Tsuchiya, Academic Press, 426 p. (1988). ISBN 0-12-385340-0.

[14] H. Duminil-Copin and S. Smirnov, *The connective constant of the honeycomb lattice equals* $\sqrt{2+\sqrt{2}}$, July 2010, preprint, `arXiv:1007.0575`.

[15] P. Fendley, *Discrete holomorphicity from topology*, talk given at the conference "Conformal Invariance, Discrete Holomorphicity and Integrability", Helsinki, June 2012.

[16] C. Hongler and K. Kytölä, *Ising interfaces and free boundary conditions*, August 2011, preprint, `arXiv:1108.0643`.

[17] Y. Ikhlef, *Discretely holomorphic parafermions and integrable boundary conditions*, J. Phys. A **45** (2012), no. 26, 265001, `http://stacks.iop.org/1751-8121/45/i=26/a=265001`.

[18] Y. Ikhlef and J. Cardy, *Discretely holomorphic parafermions and integrable loop models*, J. Phys. A **42** (2009), no. 10, 102001.

[19] M. Jimbo, *A q-analogue of $U(gl(N+1))$, Hecke algebra, and the Yang-Baxter equation* , Lett. Math. Phys. **10** (1985), 63.

[20] M. Jimbo, *Quantum R-matrix for the generalized Toda system*, Commun. Math. Phys. **102** (1986), 537–547, `doi`.

[7]In fact, such an identification is not possible for the nonchiral observable associated to H_1, *cf.* § 8.1.3.

[21] L. Mezincescu and R. I. Nepomechie, *Fractional-spin integrals of motion for the boundary sine-Gordon model at the free fermion point*, Internat. J. Modern Phys. A **13** (1998), no. 16, 2747–2764.
[22] R. I. Nepomechie, *Boundary quantum group generators of type A*, Lett. Math. Phys. **62** (2002), no. 2, 83–89.
[23] B. Nienhuis, *Critical behavior of two-dimensional spin models and charge asymmetry in the Coulomb gas*, J. Stat. Phys. **34** (1984), 731–761, `doi`.
[24] M. Rajabpour and J. Cardy, *Discretely holomorphic parafermions in lattice $\mathbb{Z}_N$ models*, J. Phys. A **40** (2007), no. 49, 14703, `http://stacks.iop.org/1751-8121/40/i=49/a=006`.
[25] V. Riva and J. Cardy, *Holomorphic parafermions in the Potts model and stochastic Loewner evolution*, J. Stat. Mech. **2006** (2006), no. 12, P12001.
[26] E. Sklyanin, *Boundary conditions for integrable quantum systems*, J. Phys. A **21** (1988), no. 10, 2375–2389.
[27] S. Smirnov, *Conformal invariance in random cluster models I. Holomorphic fermions in the Ising model*, Ann. Math. **172** (2010), no. 2, 1435–1467, `doi`.

Y. Ikhlef, M. Wheeler and P. Zinn-Justin, UPMC Univ Paris 6, CNRS UMR 7589, LPTHE, 75252 Paris Cedex, France.

R. Weston, Department of Mathematics, Heriot-Watt University, Edinburgh EH14 4AS, United Kingdom.